A novel higher-order sliding mode control for DC-DC boost converter system in PMDC motor exploring mismatched disturbances

Journal:	*Circuit World*
Manuscript ID	CW-06-2023-0144.R2
Manuscript Type:	Research Paper
Keywords:	Boost converter, higher order sliding mode, PMDC motor, sliding surface

A novel higher-order sliding mode control for DC-DC boost converter system in PMDC motor exploring mismatched disturbances

Abstract:

Purpose- The primary purpose of this article is to stabilize the rotating speed of the permanent magnet DC (PMDC) motor driven by a DC - DC boost converter under mismatched disturbances (i.e.,) under varying load circumstances like constant, frictional, fan type, propeller and undefined torques.
Design/Methodology/Approach- This manuscript proposes a higher order sliding mode control (HOSMC) to elevate the dynamic behavior of the speed controller and the robustness of the PMDC motor. A second order classical sliding surface (CSS) and proportional-integral-derivative (PIDSS) sliding surface are designed and compared.
Findings- For the boost converter with PMDC motor, both simulation and experimentation are exploited. The prototype is built for an 18W PMDC motor with field programmable gate arrays. The suggested sliding mode with second order improves the robustness of the arrangement under disturbances with a wide range of control. Both the simulation and experimental setup shows satisfactory results.
Originality/value- According to software-generated mathematical design and experimental findings, PIDSS exhibits excellent performance with respect to settling speed, steady state error and peak overshoot.

Keywords: Boost converter, higher order sliding mode, PMDC motor, sliding surface
Paper type: Research paper

Nomenclature:

SMC	- Sliding mode control
HOSMC	- Higher order SMC
PIC	- Proportional integral controller
CSS	- Classical-sliding surface
PIDSS	- Proportional–integral derivative sliding surface
PMDC motor	- Permanent magnet DC motor
D	- Relative degree
r	- Order of the sliding surface

e	- Error
n	- Order of the system
u_{eq}	- Equivalent (or) continuous term
u_{sw}	- Switching signal
C_1	- Proportional gain
C_2	- Integral gain
C_3	- Derivative gain
u	- Control signal
ω	- Angular velocity of the motor (rad/sec)
L	- Boost converter inductance (Henry)
C	- Boost converter capacitance (Farad)
i_a	- Motor armature current (Ampere)
T_L	- Load torque disturbance of the motor (Nm)
J	- Motor moment of inertia ($kg.m^2$)
v_a	- Armature voltage of the motor (Volts)
E	- Boost converter input voltage (Volts)
i_L	- Boost converter inductor current (Ampere)
K_t	- Constant of motor torque (Nm/Ampere)
K_e	- Constant of backemf of the motor (Volt/rpm)
R_a	- Motor armature resistance (Ohm)
L_a	- Motor armature inductance (Henry)
u	- Duty ratio of the boost converter
S	- Controlled switch
D_D	- Diode
PWM	- Pulse width modulation
FPGA	- Field-programmable gate array

1. INTRODUCTION

1.1 Inspiration and review of literature

DC-DC converters have been a vital component in modern and emerging applications because of their effective power transformation and management in green power systems, electric vehicles, handheld electronics, military applications, aerospace motor speed control, and advanced communication systems. The output DC voltage of these converters can be adjusted from the input DC voltage to meet the needs of the load. They are placed between the DC voltage source and the load (Mahafzah, K.A *et al.,* 2023; Babaei, E *et al.,* 2012; Babaei, E. and Seyed Mahmoodieh, M.E 2014; Babaei, E *et al.,* 2017). In a number of circumstances over the past decade, DC/DC converters, primarily buck, boost and buck-boost converters, have emerged as a new alternative actuator for DC motors (Yang, J *et al.,* 2019).

In workplaces, direct current (DC) motors are the most popular types of electrical motors. Their applications include tankers, household appliances, elevators, high-precision digital tools and robotics (Nizami *et al.,* 2022 and Li *et al.,* 2011). Additionally, DC motors are preferred over alternating current motors owing to their easy setup, a huge spectrum of speed and torque variance, and maximum electric performance (Sha *et al.,* 2017 and Crescimbini *et al.,* 2014). In the majority of DC–DC converters, the output voltage and current are modifiable so that the torque of the DC motor can be readily controlled by modifying the output voltage and current of the DC-DC converter (Asl *et al.,* 2022). The first set up of DC motor drive is a series or parallel setup of resistors combined to the DC motor.

This rheostatic regulation has a straightforward framework and is economical. In series or parallel resistors, however, a substantial amount of energy disappears as heat and large current/voltage fluctuations (Rauf *et al.,* 2021). Due to the nonlinearity of the drive, boost converters tend to be favored for industrial and commercial applications employing DC motors. Despite this, it was recently observed that boost converter-driven direct current motors have been advantageous in situations that involve regenerative deceleration in battery-powered vehicles and photovoltaic water supply (Mishra *et al.,* 2021). Boost converters require control strategies that account for model uncertainty and parameter variations. Numerous control strategies for boost converter have been recommended throughout the years (Ahmad and Ali, 2019). With regard to their basic control arrangement, simple configuration, and low expense, conventional proportional–integral (PI) derivative (PID) or proportional–integral (PI)-type controllers are the most frequent control methods in industry. The aforementioned kinds of controllers are inadequate for broader signal changes such as: abruptly introducing significant load variations (Wai and Shih, 2011). Different solutions can be found to drive the DC motor under load variations. Sliding mode - control (SMC) method is often employed to power DC-DC converters (Alonge *et al.,* 2023).

In the 1960s, pioneering work in the former Soviet Union paved the way for the development of SMC. It is a specific kind of variable structure system (VSS) with a decision rule and several feedback control laws (Spurgeon, 2014). The idea of 'variable structure system' was initially coined in the late 1950s. Then, recent control issues, modern computational techniques and current advancements in switching circuitry result in the emerging of new control principles (Utkin, 1993). A system with SMC features has the primary benefit of being guaranteed stable and resistant against parameter uncertainty. When it is compared to other nonlinear control systems, the SMC method is one of the easiest methods to apply. With any of these characteristics, SMC is well suited for nonlinear systems, which is exhaustively adopted in industrial usage including: electrical drives, converters, automotive systems. furnace control etc., (Tan, Lai and Tse, 2018). Table I. shows the survey of SMC relating to various applications with challenges addressed.

Despite asserted durability characteristics, the ensuing controller has a particular deficiency. The limitation is the chattering phenomenon, or vibrations at high frequencies of the regulated setup, which diminish the behavior and contribute to unreliability. Retaining the primary benefits of conventional SMC, a method known as higher order SMC (HOSMC) has been pitched to reduce the phenomenon of chattering. For maintaining stability in highly non-linear systems, HOSMC is particularly effective. HOSMC can provide more flexibility and better performance when the control objectives are complex and involves different objectives or restrictions. It is robustness to uncertainties, disturbances, and variations in system parameters. Chattering, a common problem in basic sliding mode control, can be reduced or eliminated by advanced sliding mode control methods such as: HOSMC. HOSMC is frequently used in specialized applications like aerospace, robotics, electric drives, etc. where precise control is essential. In favour of affecting the initial time derivative sliding variable, the signum function influences the time derivative with higher order (Defoort *et al.,* 2009).

Table I. Survey of SMC relating to various applications with challenges addressed

Authors. (Year)	Topology	Type of Sliding mode	Load	Challenges addressed	Disadvantages
Waghmare and Chaturvedi (2023)	Flyback converter	Higher order SMC	Solar PV based applications	Chattering reduction	In comparison to first-order SMC, higher-order SMC may involve a greater control effort (e.g., larger control inputs)
Malge *et al.,* (2023)	Interleaved boost converter	Non-singular fast terminal SMC	Resistive load	Voltage regulation under disturbances	More complex to design and implement in comparison with traditional SMC. It requires a deeper understanding of system dynamics
Rivera *et al.,* (2023)	boost converter	second order SMC	Resistive load	Robust performance under parameter variations	Selection of perfect gains can be difficult and time-consuming
Zambrano-Prada *et al.,* (2023)	boost converter	SMC with polynomial sliding surface	Constant power load	Disturbance rejection, inrush current, stability	Higher computational complexity
Appikonda and Kaliaperumal, (2022)	Dual input boost converter	Double integral SMC	Resistive load	Regulation in voltage under input and load disturbances	Sluggish transient response
Corradini, Ippoliti and Orlando, (2022)	Discontinuous boost converter	Load estimation sliding mode observer	Resistive load	Tested under parameter variations	Low estimation accuracy
Inomoto, Monteiro and Filho, (2022)	boost converter	SMC with integrative sliding surface	Resistive load	Reduces steady state error, peak overshoot	Design complexity
Pandey *et al.,* (2021)	Fuel cell-based boost converter	SMC	PMDC motor	Speed variation	Undesired high frequency oscillations
Wu and Lu, (2019)	boost converter	Adaptive backstepping SMC	Constant power load	Improves the stability of the DC bus voltage	Complex for nonlinear system having coupled dynamics

Chincholkar, Jiang and Chan, (2018)	Cascade boost converter	PWM based SMC	Resistive load	Improves the output voltage response	Selecting an inappropriate frequency may lead to undesirable effects, such as: increased switching losses or harmonic distortion
Aydogmus, Deniz and Kayisli, (2014)	boost converter	SMC	permanent magnet synchronous motor	Power factor correction	Undesired high frequency oscillations
Oucheriah, (2014)	boost converter	Adaptive SMC	Resistive load	Output voltage regulation	Tuning the adaptive laws and control gains
Kumar and Jeevananthan, (2012)	Negative Output elementary boost converter	Hysteresis SMC	Resistive load	Wide variations in line, and load	Introduces nonlinear behavior into the system

Sliding mode control can be incorporated into electric vehicles through a variety of methods. Pisano *et al.,* 2008 proposed a cascade control mechanism that uses a 2nd-order SMC algorithm to facilitate the speed/position control of permanent-magnet DC (PMDC) motor drives. This strategy offers precise performance under significant motor and load parameter uncertainty in a commercial PMDC motor drive. (Feng *et al.,* 2020) proposed a novel SMC that is applied for the drives with permanent magnet synchronous motor for the speed regulation. Various higher order sliding surfaces are presented for the speed regulation of PMDC motor with different load torques (Ravikumar and Srinivasan, 2022).

1.2 Contribution and the structure of the paper

Despite the presence of various disturbances/uncertainties, a thorough control strategy for DC motor smooth starters that takes care of speed regulation is still required. From the preceding discussions, in this work, a novel higher order SMC method for the PMDC motor speed regulation system driven by the boost converter under various load circumstances. A control strategy known as proportional-integral-derivative sliding surface (PIDSS) control combines the principles of sliding mode control with traditional PID control to achieve improved performance. To ensure that the system accurately reaches and maintains the desired setpoint, the integral component of PIDSS eliminates steady-state errors. This is crucial for applications where precise control is necessary. In comparison to sliding mode control, higher order PIDSS control can offer smoother control action, lowering the risk of chattering and mechanical component wear and tear.

The paper's most important contributions are furnished below:

- Generalized procedure for HOSMC is designed
- Design of PI derivative sliding surface (PIDSS) with second order time derivative and second order classical-sliding surface (CSS) are completed
- Simulation work is carried out using proportional integral controller (PIC), SMC, CSS with second order time derivative and PIDSS with second order time derivative under a variety of load conditions including constant, frictional, fan type, propeller and undefined
- Real-time implementation of HOSMC for PMDC motor powered by boost converter
- Recommended control method reduces over-shoot, dismisses disturbance, possesses an adequate level of control excellence over a wider operating range, and is more resistant to unpredictability.

The sequence of the chapters in this paper are as follows:

Standard practice for designing HOSMC is described in the second section. In the third section, modeling of the PMDC motor powered by a boost converter is discussed. The fourth section describes how HOSMC design is made and the procedure for designing CSS and PIDSS are done. The findings from the simulations are laid out in the fifth portion, which demonstrates the robustness of the HOSMC and the experimental study and performance validation are examined in the sixth section. The seventh section concludes with the recommendations for the future.

2. GENERALIZED PROCEDURE FOR DESIGNING HOSMC

The general HOSMC implementation process is described in this section. The control signal for a PMDC motor powered by boost converter with a classical sliding surface and PID sliding surface is proposed on the basis of a generalized procedure. The HOSMC is built using a sliding surface and a suitably designed control signal so that the state trajectories can reach and reside on the sliding surface. Following is a description of the general procedure for creating control law with higher order SMC.

Step 1: System Description

Consider a 'n^{th}' order system with 'x_n' as output variable and it is represented by a set of expressions as shown in (1).

$$\frac{dx_1}{dt} = a_{11}x_1(t) + a_{12}x_2(t) + \ldots\ldots + a_{1n}x_n(t) + b_{1n}u(t)$$

$$\frac{dx_2}{dt} = a_{21}x_1(t) + a_{22}x_2(t) + \ldots\ldots\ldots\ldots + a_{2n}x_n(t)$$

……

$$\dot{x}_n = a_{n1}x_1(t) + a_{n2}x_2(t) + \ldots\ldots\ldots + a_{nn}x_n(t) \quad (1)$$

Where $x_1(t), x_2(t)\ldots\ldots\ldots x_n(t)$ be the state variables, u(t) is the control variable and a_{ij} are constant parameters, where i= 1, 2,….n and j=1,2,…..n. In order to construct a higher order SMC for the output variable 'x_n', it is necessary to fix the order of the sliding surface through relative degree calculation. Relative Degree (D) of a system can be identified by the step number at which step by step differentiation of the output variable brings control input into

the calculation. After computing relative degree, order of the sliding surface (r) is calculated by computing 'D-1'.

Step 2: Identification of relative degree

The relative degree (D) of 'n^{th}' order system is calculated through differentiating the output parameter $'x_n(t)'$ repeatedly until the control signal 'u' reaches. The earliest derivative of the output term $'x_n(t)'$ is represented as follows:

$$\frac{dx_n}{dt} = f(x_n) + \text{constant term} \quad (2)$$

The second and subsequent derivatives of the output term $'x_n(t)'$ are given as,

$$\frac{d^{D-(n-2)}x_n}{dt^{D-(n-2)}} = f^{i=1}(x_n) + f(x_n) + \text{constant term} = f^{I}(x_n) + f(x_n) + \text{constant term} \quad (3)$$

$$\frac{d^{D-(n-3)}x_n}{dt^{D-(n-3)}} = f^{i=D-(n-2)}(x_n) + f^{i=1}(x_n) + \text{constant term} = f^{II}(x_n) + f^{I}(x_n) + \text{constant term} \quad (4)$$

$$\frac{d^{D}x_n}{dt^{D}} = f^{i=D}(x_n) + b_{1n}u + \text{constant term} \quad (5)$$

At D^{th} time derivative $(D \leq n)$, the control input 'u' appears which verifies the system's relative degree as 'D'. From this, the order of the sliding surface can be calculated by using the formula (D-1).

Step 3: Sliding surface and its derivatives

To design the HOSMC for the output variable $'x_n'$, the intended goal is to impose a r^{th} order sliding mode upon S(e,ė) =0. If S(e,ė) is the sliding surface consisting of a linear combination of state variables.

i.e., $S(e,\frac{de}{dt}) = \dot{S}(e,\frac{de}{dt}) = \ldots\ldots S^{r-1}(e,\frac{de}{dt}) = 0$

Where $e = x_n - x_d$, taken as an error. $'x_n'$ is the precise output term and $'x_d'$ represents the set output term.

The initial differentiation of S(e,ė) can be written as,

$$\dot{S}(e,\dot{e}) = \frac{\partial S(e,\dot{e})}{\partial X_n} = f^{I}(e,\dot{e}) + \text{constant term} \quad (6)$$

The subsequent derivative of S(e,ė) appears as outlined below:

$$\ddot{S}(e,\dot{e}) = \frac{\partial^2 S(e,\dot{e})}{\partial {X_n}^2} = f^{II}(e,\dot{e}) + f^{I}(e,\dot{e}) + \text{constant term} \quad (7)$$

……

$$\overset{D-1}{S}(e,\dot{e}) = \frac{\partial^{D-1} S(e,\dot{e})}{\partial {X_n}^{D-1}} = f^{D-1}(e,\dot{e}) + f^{D-2}(e,\dot{e}) + \ldots..f^{I}(e,\dot{e}) + b_{1n}u + \text{constant term} \quad (8)$$

The control input 'u' appears at the sliding order (D-1).

Step 4: Generation of equivalent (continuous) signal 'u_{eq}'

Determine the equivalent i.e., continuous term 'u_{eq}' via the derivatives of $S(e,\frac{de}{dt})$. The control signal 'u' is shown in (9).

$$\overset{D-1}{S(e,\dot{e})} = f^{D-1}(e,\frac{de}{dt}) + f^{D-2}(e,\frac{de}{dt}) + \ldots\ldots f^{I}(e,\frac{de}{dt}) + b_{1n}u + \text{constant term} = 0 \qquad (9)$$

Making $\overset{D-1}{S(e,\dot{e})} = 0$ and replacing 'u' as 'u_{eq}', then the sliding surface equation will be written as,

$$u_{eq} = [f^{D-1}(e,\frac{de}{dt}) + f^{D-2}(e,\frac{de}{dt}) + \ldots\ldots\ldots f^{I}(e,\frac{de}{dt}) + \text{constant term}]\,[b_{1n}]^{-1} \qquad (10)$$

In the state equations of the boost converter fed PMDC motor, the constant term is fixed as "Load torque disturbance of the motor - T_L (Nm)". In the control aspect, the equivalent signal 'u_{eq}' is generated by making the second derivative of the sliding surface to zero. The equivalent signal 'u_{eq}' consists of the constant term i.e., "Load torque disturbance of the motor - T_L (Nm). Two scenarios of control are arising in the equivalent signal 'u_{eq}' with respect to the constant term "Load torque disturbance of the motor - T_L (Nm)'.

Scenario i: When the constant term "Load torque disturbance of the motor - T_L (Nm)' is zero i.e., at no load conditions.

Scenario ii: When the constant term "Load torque disturbance of the motor - T_L (Nm)' is non zero i.e., during loaded conditions.

The value of the equivalent signal 'u_{eq}' is changed depending upon the speed reference and the constant term T_L (Nm). If the equivalent signal 'u_{eq}' is changed, then the control signal 'u' also be changed because $u = 'u_{eq}' + 'u_{sw}'$. So that the effective and robust control action is attained here.

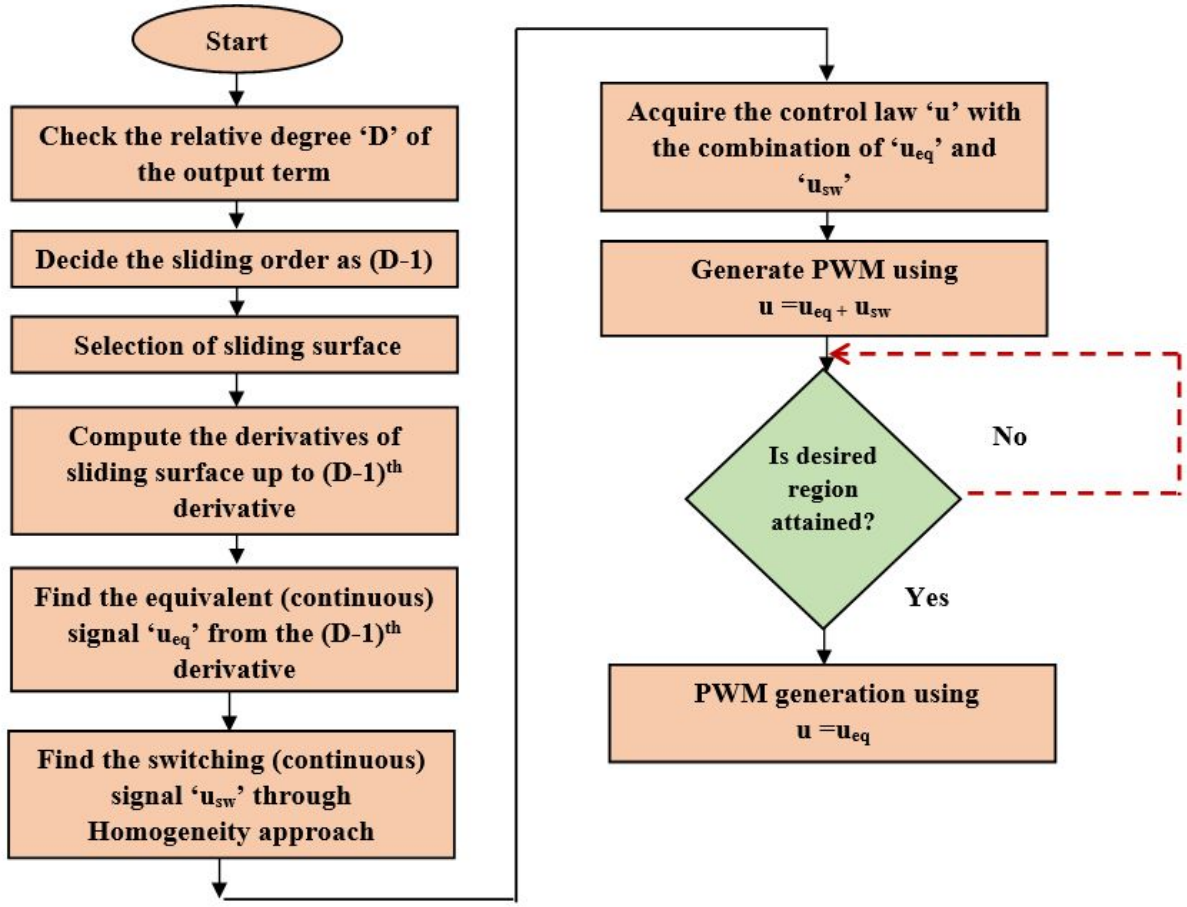

Figure 1 Flowchart representation of HOSMC design

Step 5: Selection of switching signal $'u_{sw}'$

The switching signal $'u_{sw}'$ is obtained by the following general equation (11) (Levant, 2005),

$$N_{ir} = \{|S|^{q/r} + \left|\frac{dS}{dt}\right|^{q/r-1} + ... + \left|(S^{i-r})\right|^{q/r-i+1}\}^{(r-i/q)} \quad (11)$$

where,

The least common divisor (or) multiple of 1 to r is q, where 'r' is the sliding order and i= 1……(r-1).

$$\varphi_{0r} = \text{sign}\,(S) \quad (12)$$

$$\varphi_{ir} = \text{sign}(S^{(i)} + \beta_i N_{ir}\varphi_{i-1,r}) \quad (13)$$

The switching signal for the r^{th} order sliding controller is given as,

$$u_{sw} = -\alpha\,\varphi_{r-1,r}\,(S, \dot{S}.....S^{r-1}) \quad (14)$$

Select the control parameters $\alpha > 0\ and\ \beta_i > 0$, such that to make the scheme to sustain in a finite amount of time.

Step 6: Final control law

Compute the conclusive control signal $\{u = u_{eq} + u_{sw}\}$, employing two cumulative parameters; the continuous parameter $'u_{eq}'$ and the discontinuous parameter $'u_{sw}'$. The control signal 'u' for the CSS is outlined as follows,

$$u_{CSS} = [-[f^{D-1}(e,\dot{e}) + f^{D-2}(e,\dot{e}) + \ldots\ldots f^{1}(e,\dot{e}) + \text{constant term}]\,[b_{1n}]^{-1}] + u_{sw} \quad (15)$$

Finally, the control signal 'u' for PIDSS is expressed as,

$$u_{PIDSS} = [-[D_1(\dot{e}) + D_2(e) + D_3(\ddot{e})\ \text{constant term}]\,[b_{1n}]^{-1}] + u_{sw} \quad (16)$$

Figure 1 shows the flowchart representation for designing HOSMC.

3. MODELLING OF PMDC MOTOR POWERED BY DC-DC BOOST CONVERTER

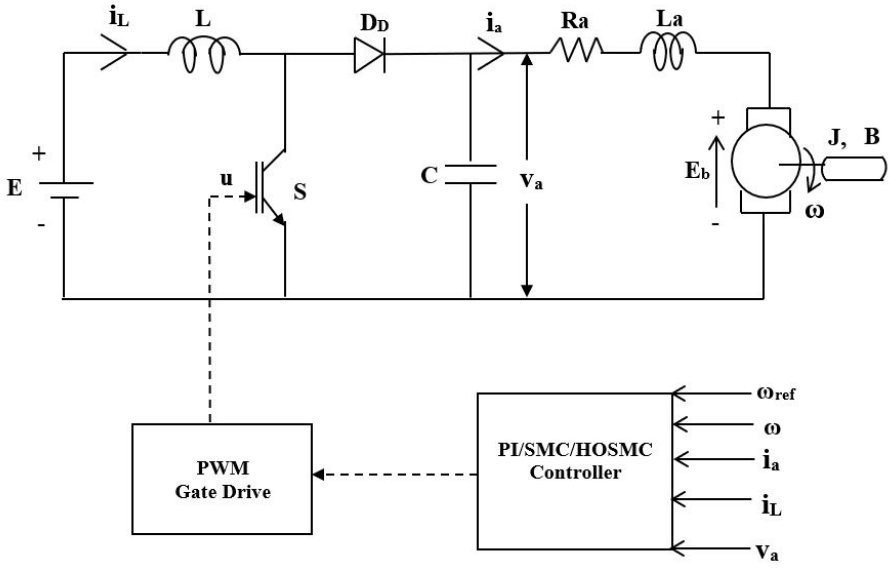

Figure 2 Diagram for PMDC motor powered by boost converter

The implementation of servo and regulatory operation of the PMDC motor powered by boost converter using the PIC, SMC and second order SMC using CSS and PIDSS are shown in Figure 2. Additionally, it aims to contrast the responsiveness of the aforementioned controllers with the inclusion of loaded and unloaded scenarios. The following is the mathematical description of the proposed scheme using the boost converter with PMDC motor.

$$\frac{di_L}{dt} = -(1-u)B_7 v_a + B_7 E u$$

$$\frac{dv_a}{dt} = -B_4 i_a + (1-u)B_4 i_L$$

$$\frac{di_a}{dt} = -B_6 \omega - B_2 i_a + B_5 v_a$$

$$\frac{d\omega}{dt} = -B_3 \omega + B_1 i_a - B_8 T_L \quad (17)$$

where,

$$B_1 = \frac{K_t}{J};\ B_2 = \frac{R_a}{L_a};\ B_3 = \frac{B}{J};\ B_4 = \frac{1}{C};\ B_5 = \frac{1}{L_a};\ B_6 = \frac{K_e}{L_a};\ B_7 = \frac{1}{L};\ B_8 = \frac{1}{J}$$

The parmeters of PMDC motor powered by boost converter are as follows:

- ω Angular velocity of the motor (rad per sec)
- L Boost converter inductance (Henry)
- C Boost converter capacitance (Farad)
- i_a Motor armature current (Ampere)
- T_L Load torque disturbance of the motor (Nm)
- J Motor moment of inertia ($kg.m^2$)
- v_a Armature voltage of the motor (Volts)
- E Boost converter input voltage (Volts)
- i_L Boost converter inductor current (Ampere)
- K_t Constant of motor torque (Nm/Ampere)
- K_e Constant of backemf of the motor (Volt/rpm)
- R_a Motor armature resistance (Ohm)
- L_a Motor armature inductance (Henry)
- u duty ratio of the boost converter
- S controlled switch
- D_D Diode

3.1 Identification of SMC Order

It is essential to compute the proposed system's relative degree 'D' in order to determine the SMC order. Calculating the relative degree, differentiate the output term (speed) continuously until control input 'u' reaches. The procedure is explained below from the Equation (18) to Equation (23).

$$\dot{\omega} = -B_3\omega + B_1 i_a - B_8 T_L \tag{18}$$

On differentiating the Equation (18) further, Equation (19) is obtained as,

$$\ddot{\omega} = -B_3\dot{\omega} + B_1\dot{i_a} - B_8\dot{T_L} \tag{19}$$

Put the Equation (18) and the value of $'\dot{i_a}'$ in Equation (19), then the following expression are obtained.

$$\ddot{\omega} = -B_3(-B_3\omega + B_1 i_a - B_8 T_L) + B_1(-B_6\omega - B_2 i_a + B_5 v_a) \tag{20}$$

$$\ddot{\omega} = \omega(B_3B_3 - B_1B_6) + i_a(-B_3B_1 - B_1B_2) + v_a(B_1B_5) + B_3B_8T_L \tag{21}$$

Differentiating the Equation (21) further with respect to 't' will gives,

$$\dddot{\omega} = \dot{\omega}(B_3B_3 - B_1B_6) + \dot{i_a}(-B_3B_1 - B_1B_2) + \dot{v_a}(B_1B_5) + B_3B_8\dot{T_L} \tag{22}$$

Put the values of $'\dot{\omega}'$, $'\dot{i_a}'$ and $'\dot{v_a}'$ in Equation (22),

$$\ddot{\omega} = (-B_3\omega + B_1 i_a - B_8 T_L)(B_3B_3 - B_1B_6) + (-B_6\omega - B_2 i_a + B_5 v_a)(-B_3B_1 - B_1B_2) + (-B_4 i_a + (1-u)B_4 i_L)(B_1B_5) \quad (23)$$

The third derivative of the output term in Equation (23), which contains the control parameter "u" has a relative degree "D" of three as a result. This implies that it is possible to obtain the 2nd order SMC.

4. CONTROLLER DESIGN

The primary goal of the design structure is to diminish the amount of time required for the angular motion of the motor to reach the desired equilibrium place.

4.1 Design of second order SMC with CSS

Equation (24) represents CSS,

$$\rho = Ce + \frac{de}{dt} \quad (24)$$

where 'e' is the error of the motor speed i.e., deviation between actual 'ω' and reference speed 'ω_{rs}'. C is the real value.

$$\rho = C(\omega_{rs} - \omega) - \frac{de}{dt} \quad (25)$$

$$\rho = C(\omega_{rs} - \omega) + B_3\omega - B_1 i_a + B_8 T_L \quad (26)$$

The initial derivative of $'\rho'$ is,

$$\frac{d\rho}{dt} = ((\omega Z_1) + (i_a Z_2) - (B_1B_5v_a) + (T_L Z_3)) \quad (27)$$

where,

$$Z_1 = ((CB_3) - (B_3^2) + (B_1B_6))$$

$$Z_2 = ((B_3B_1) - (CB_1) + (B_1B_2))$$

$$Z_3 = ((CB_8) - (B_3B_8))$$

The next derivative of $'\dot{\rho}'$ is,

$$\frac{d}{dt}\left(\frac{d\rho}{dt}\right) = ((\omega Z_4) + (i_a Z_5) + (v_a Z_2 B_5) + (uB_1B_5B_4i_L) - (T_L B_8 Z_1)) \quad (28)$$

where,

$$Z_4 = (-(B_3Z_1) - (B_6Z_2))$$

$$Z_5 = ((B_1Z_1) - (B_2Z_2) - (B_1B_5B_4))$$

The equivalent signal is generated by making $\ddot{\rho} = 0$ and u as $'u_{eq}'$ in the Equation (28). Now the equivalent signal is given as in the Equation (29),

$$u_{eq} = -[\omega Z_4 + i_a Z_5 + v_a Z_2 B_5 - T_L B_8 Z_1]/i_L B_1 B_5 B_4 \quad (29)$$

For the second order SMC, the switching signal generation is given as (Levant, 2005),

$$N_{ir} = (|\delta|^{q/r} + |\dot{\delta}|^{q/r-1} + ... + |(\delta^{i-r})|^{q/r-i+1})^{(r-i/q)} \quad (30)$$

where, q is the least common multiple of 1….r, where 'r' is the sliding order and i= 1……(r-1).

$$\varphi_{0r} = \text{sign}\,(\delta) \quad (31)$$

$$\varphi_{ir} = \text{sign}(\delta^{(i)} + \beta_i N_{ir} \varphi_{i-1,r}) \quad (32)$$

The switching signal for the r^{th} order sliding controller is given as,

$$u_{sw} = -\alpha\, \varphi_{r-1,r}\, (\delta, \dot{\delta} .....\delta^{r-1}) \quad (33)$$

The sliding mode with r^{th} order is defined by $\delta = \dot{\delta} = ...\delta^{r-1} = 0$.

For second order SMC, r= 2, so that the value of i= 1. Let q be taken as 2.

Substitute the values of 'r', 'q' and 'i' in the Equations (30), (31), (32) and (33), then it leads to,

$$N_{12} = (|\delta|)^{(1/2)} \quad (34)$$

$$\varphi_{02} = \text{sign}\,(\delta) \quad (35)$$

$$\varphi_{12} = \text{sign}\,(\dot{\delta} + \beta_1 N_{12} \varphi_{02}) \quad (36)$$

The switching signal for the 2^{nd} order SMC is given as,

$$u_{sw} = -\alpha\, \varphi_{12} \quad (37)$$

Substitute the Equations (34), (35) and (36) in (37), the switching signal is obtained as,

$$u_{sw} = -\alpha(\text{sign}\,(\dot{\delta} + \beta_1((|\delta|)^{(1/2)})(\text{sign}\,(\delta)\,))) \quad (38)$$

The final control law is the combination of equivalent signal and switching signal. The final control law is given as in the Equation (39),

$$u_{CSS} = \{-[\omega Z_4 + i_a Z_5 + v_a Z_2 B_5 - T_L B_8 Z_1]/i_L B_1 B_5 B_4\} + \{-\alpha(\text{sign}\,(\dot{\delta} + \beta_1((|\delta|)^{(1/2)})(\text{sign}\,(\delta)\,))\} \quad (39)$$

In the 2nd-order CSS, the sliding factor 'C' is set to 5 using the approach of trial and error (Komurcugil,H, et al., 2021) so that the speed tracking profile is satisfactory and disturbance-free. To ensure that the control strategy stays consistent and confined within 1, the control parameters α and β_1 are selected as $50*10^{50}$ and 1500.

4.2 Design of second order SMC with PIDSS

Here, sliding surfaces are selected based on proportional-integral-derivative parameters to control the PMDC motor speed against a variety of load torque circumstances.

$$\text{error} = e = \omega_{rs} - \omega \tag{40}$$

Now PIDSS has been designated as,

$$\varphi = C_1 e + C_2 \int e dt + C_3 \frac{de}{dt} \tag{41}$$

where C_1, C_2 and C_3 are the proportional -integral-derivative gains

$$\varphi = C_1(\omega_{ref} - \omega) + C_2 \int (\omega_{ref} - \omega) dt - C_3(-B_3\omega + B_1 i_a - B_8 T_L) \tag{42}$$

The initial derivative of the equation (42) is,

$$\frac{d\varphi}{dt} = \omega Z_1 + i_a Z_2 + v_a Z_3 + D_2(\omega_{rs} - \omega) + T_L(C_1 B_8 - C_3 B_3 B_8) \tag{43}$$

where,

$$Z_1 = (C_1 B_3 - C_3 B_3^2 + C_3 B_1 B_6)$$

$$Z_2 = (-C_1 B_1 + C_3 B_3 B_1 + C_3 B_2 B_1)$$

$$Z_3 = (C_3 B_1 B_5)$$

The next derivative of $'\frac{d\varphi}{dt}$, is,

$$\frac{d}{dt}\left(\frac{d\varphi}{dt}\right) = \omega Z_4 + i_a Z_5 + v_a Z_6 + i_L u B_4 + T_L Z_7 \tag{44}$$

where,

$$Z_4 = (-B_3 Z_1 - B_6 Z_2 + C_2 B_3)$$

$$Z_5 = (B_1 Z_1 - B_2 Z_2 - B_4 Z_3 - C_2 B_1)$$

$$Z_6 = (B_5 Z_2)$$

$$Z_7 = (C_2 B_8 - B_8 Z_1)$$

The equivalent signal is generated by making $\ddot{\varphi} = 0$ and u as $'u_{eq}'$ in the Equation (44). Now the equivalent signal is represented in Equation (45),

$$u_{eq} = -[\omega Z_4 + i_a Z_5 + v_a Z_6 - T_L Z_7\ ]/\ i_L B_4 \tag{45}$$

For the second order SMC, the switching signal is given as in the Equation (46),

$$u_{sw} = -\alpha(\text{sign}\ (\dot{\varphi} + \beta_1((|\varphi|)^{(1/2)})(\text{sign}\ (\varphi)\ ))) \tag{46}$$

To reach the sliding surface to '0', the parameters of α and β_1 are considered as real positive coefficients. The values of C_1, C_2 and C_3 are chosen as 8, 0.25 and 0.5 respectively. The control parameters α and β_1 are $50*10^{25}$ and 1500, respectively.

The final control law is the combination of equivalent signal and switching signal. The final control law is given as in the Equation (47),

$$u_{PIDSS} = \{ - [\omega Z_4 + i_a Z_5 + v_a Z_6 - T_L Z_7]/ i_L B_4 \} + \{ - \alpha(\text{sign}(\dot{\varphi} + \beta_1((|\varphi|)^{(1/2)})(\text{sign}(\varphi))) \} \quad (47)$$

5. SIMULATION RESULTS AND DISCUSSIONS

Table II. Specifications of boost converter with PMDC motor and the machine behaviour

Parameter	Symbol	Value
Boost converter input voltage	E	4V
Converter inductance	L	2mH
Converter capacitance	C	1000μF
Converter switching frequency	F	10 kHz
Converter Switch	S	-
Converter Diode	D_D	-
Motor power	P_o	18W
Motor armature voltage	V_a	12V
Motor armature current	I_a	1.5A
Motor torque	T	1 kG.cm
Motor armature resistance	R_a	2.6 Ω
Motor armature inductance	L_a	712.85 mH
Backemf constant	K_e	0.05022 Vs/rad
Moment of Inertia	J	8.86138e-5 kg.m^2
Viscous friction coefficient	B	9.6894e-5 Nm/rad
Torque constant	K_e	0.05022 Nm/A
Speed	ω	157 rad/sec
Machine behaviour		
Time (secs)	**Speed reference pattern (p.u.)**	**Load torque pattern (p.u.)**
0 to 4 seconds	0.5	-
4 to 6 seconds	0.5	0.5
6 to 8 seconds	1	0.5
8 to 10 seconds	1	1
10 to 11 seconds	0.6	1

With the suggested system, the effectiveness of PIC, SMC and CSS and PIDSS under second order is examined. The recommended HOSMC is confirmed by using Matlab simulation for varying torque constraints with the configurations reported in Table II. The general law serves as the direct framework for the conventional approach to achieving SMC. So, the switching signal for SMC is,

$$u = 0.5(1 - \text{signum}(\text{sliding surface})) \quad (48)$$

Sliding surface is the error signal. Whenever the control signal is explicitly applied, it leads the framework of the system to toggle both on on/off at extreme frequencies, resulting in unforeseen chattering. In HOSMC, the sliding surface with second order is employed to disable chattering and to ensure effortless operation of the PMDC motor. The behaviour of PIC, SMC, higher order CSS, higher order PIDSS are tested for various loading situations.

Case 1: Robustness under constant load circumstances

The consistency of the controllers is tested under a range of load torques, including frictional, fan, propeller, and constant loads. Table II lists the specifications of the machine's behavior for the opted speed and load torque pattern. Figure 3 and Figure 4 display the chosen speed and load torque appearance, respectively.

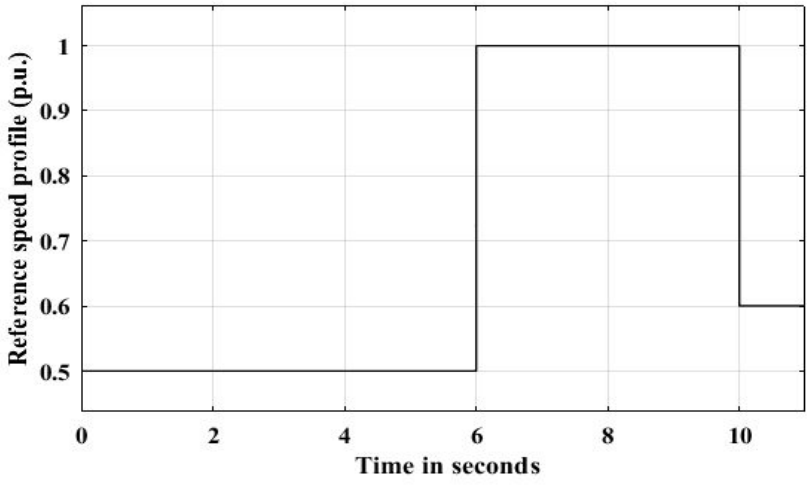

Figure 3 Speed reference pattern

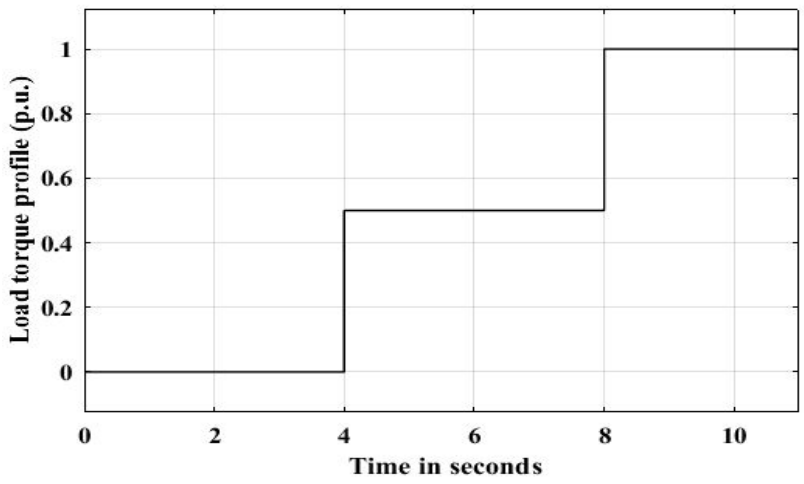

Figure 4 Load torque pattern

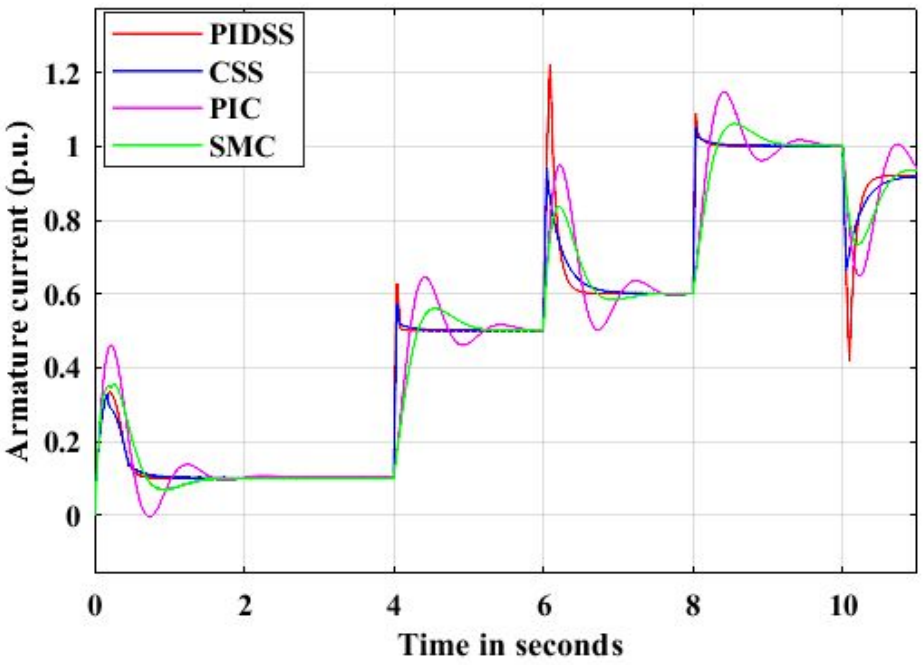

Figure 5 Comparison of armature current between PIC, SMC, second order SMC using CSS and PIDSS for the torque at constant load

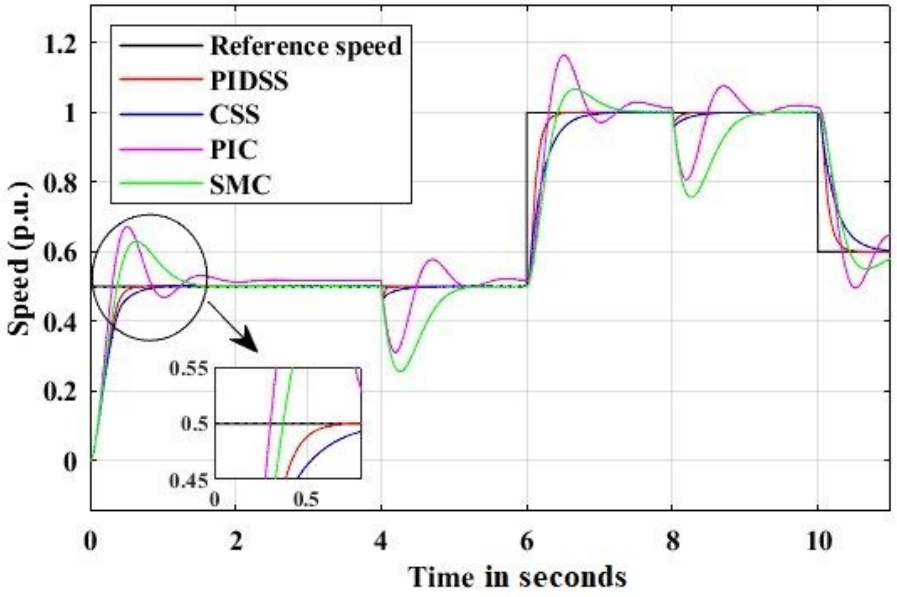

Figure 6 Inspection of the speed response of PIC, SMC, second-order SMC with CSS and PIDSS for the torque at constant load

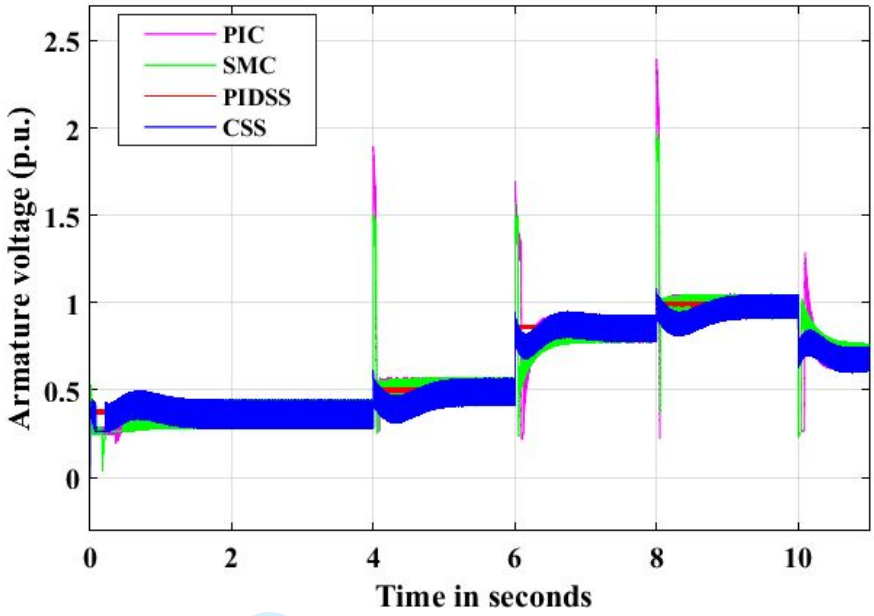

Figure 7 Inspection of the armature voltage response of PIC, SMC, second-order SMC with CSS and PIDSS for the torque at constant load

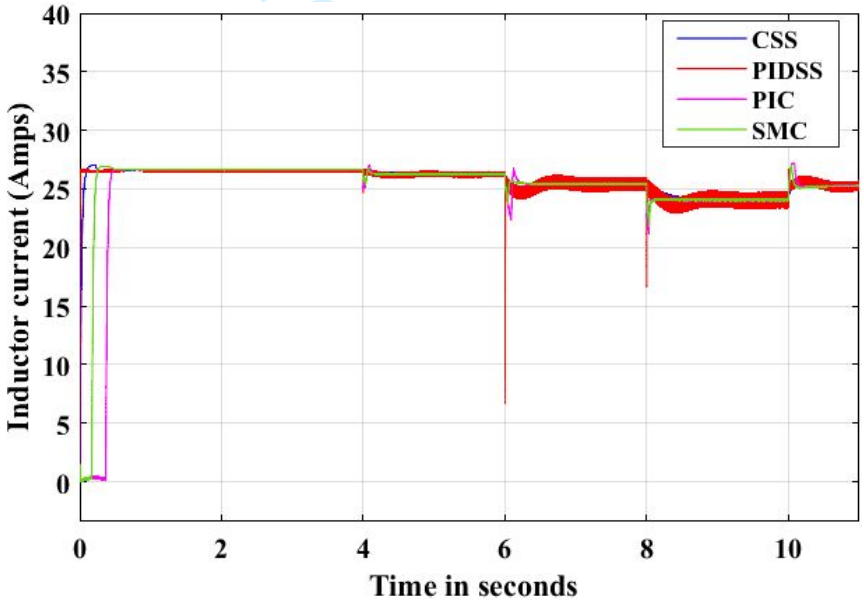

Figure 8 Inspection of the inductor current response of PIC, SMC, second-order SMC with CSS and PIDSS for the torque at constant load

For constant load torque situations, the simulation outcomes for PIC, SMC, second order SMC using CSS and PIDSS are compared. The responses of second order SMC using PIDSS over second order SMC with CSS is better on the basis of recovery period, disturbance suppression, peak overshoot, and steady-state error. The convergence of the sliding surface of second order SMC with PIDSS is compared with second order SMC with

CSS without steady state error. In contrast to PIC, SMC, and second order SMC with CSS for the load torque pattern, as displayed in Figure 4, the speed of the PMDC motor is quickly stabilized in the absence of squealing by second order SMC using PIDSS. Figure 5 and Figure 6 shows the computational outcomes for the comparison study of armature current progressions and speed for the load torque with constant scenario with the ranges of speed and load torque as depicted in Table III. Figure 6 contrasts the settling times for constant load torque circumstances for PIC, SMC, second order SMC using CSS and PIDSS. Figures 7 and 8 illustrate the armature voltage and inductor current responses of the boost converter under constant load torque conditions. The response of both armature voltage and inductor current exhibits a smoother behaviour when employing second-order SMC with PIDSS, as compared to PIC, SMC, and second-order SMC with CSS. According to the above findings, second order SMC with PIDSS serves far superior than PIC, SMC, and second order SMC using CSS.

Case 2: Robustness under the torque due to frictional load

For the torque due to frictional load, $T_L = K_1\omega$. K_1 is taken as the proportional representation constant ($3.8e^{-4}$), so that the load torque stays in the acceptable range. Figure 9 illustrates the load torque reference pattern for the speed reference in Figure 3. Figure 10 illustrates that second order SMC using PIDSS has a faster settling time for PMDC motor speed than PIC, SMC, and second order SMC using CSS. In Figure 10, peak overshoot occurs in SMC and PIC during the period 0 seconds to 4 seconds and steady state error occurs in PIC and it is shown in the Table III.

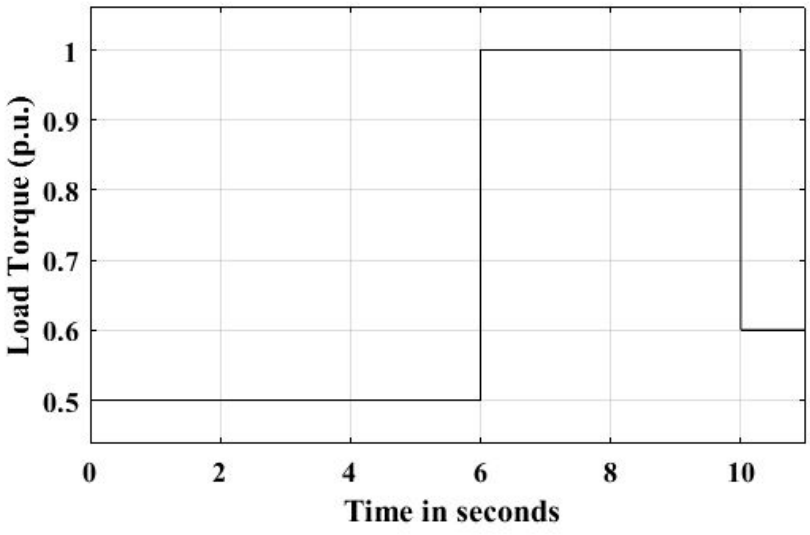

Figure 9 Torque due to frictional load - ($T_L \alpha \omega$)

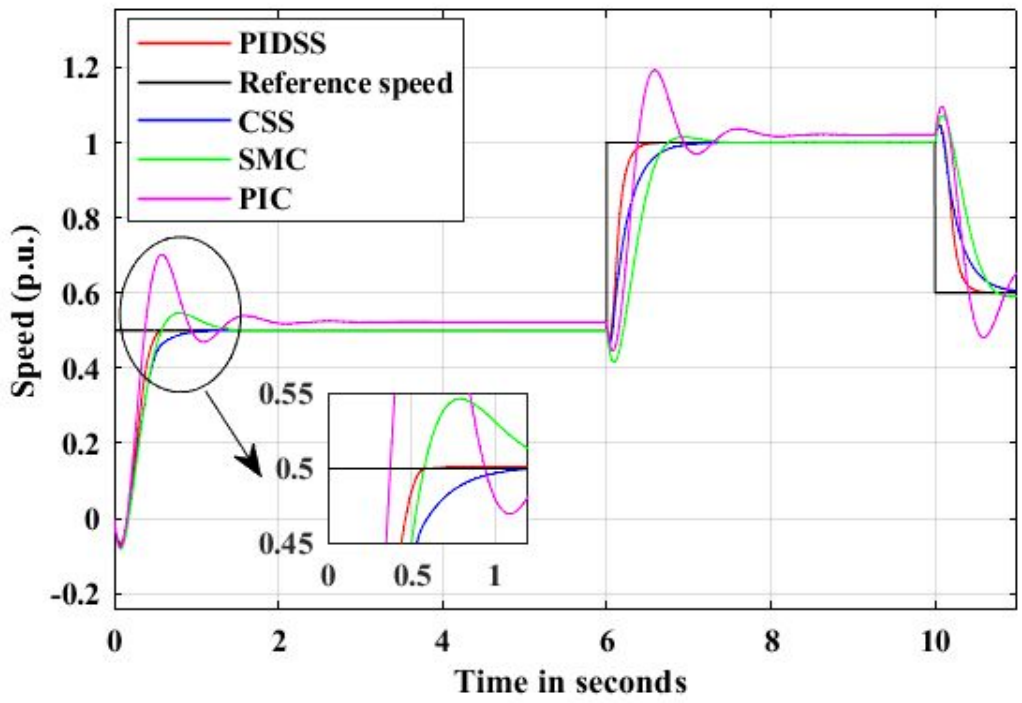

Figure 10 Speed response comparative study between PIC, SMC, second order SMC using CSS and PIDSS over frictional load torque

Case 3: Robustness under the torque due to fan type load

For the torque due to fan type load, $T_L = K_2\omega^2$. K_2 is opted to have a proportional representation constant value of $2.44e^{-6}$. Figure 11 depicts fan type load torque for the speed reference pattern indicated through Figure 3.

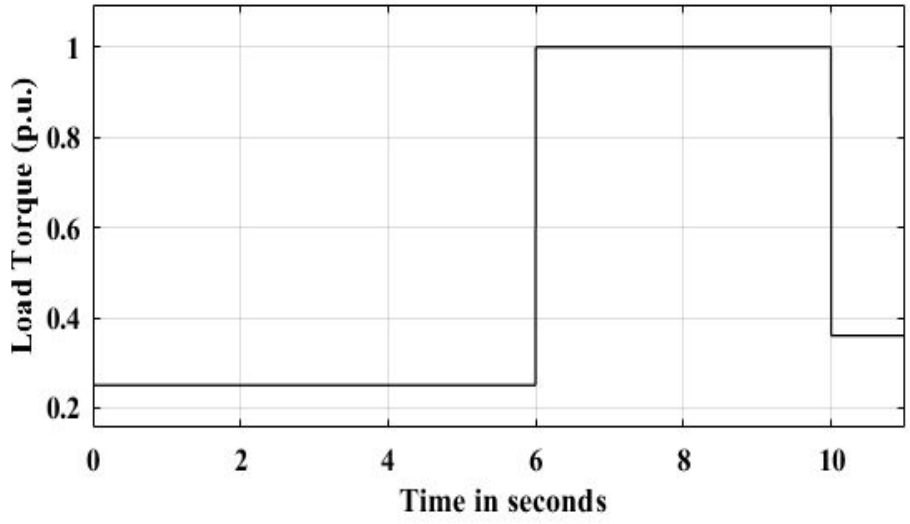

Figure 11 Torque due to fan type load - (T_L α ω^2)

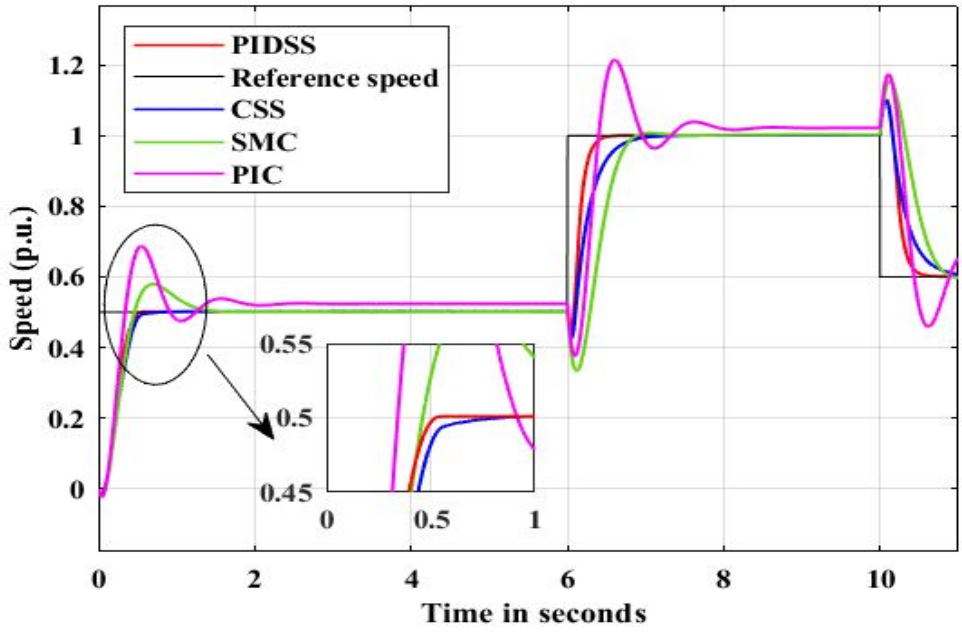

Figure 12 Speed response correlation between PIC, SMC, second order SMC using CSS and PIDSS for the torque due to fan type load

Figure 12 demonstrates that the ability to resolve the speed performance of the PMDC motor is more robust for second order SMC with PIDSS than for second order SMC with CSS, SMC, and PIC. During the initial period, both PIC and SMC exhibit peak overshoot. The details of peak overshoot, steady state error and settling duration of PIC, SMC and second order CSS and PIDSS is shown in Table III.

Case 4: Robustness under the torque due to propeller type load

For the torque due to propeller type load, $T_L = K_3\omega^3$. The value of the proportionality constant K_3 was found to be $1.55e^{-8}$. Figure 13 depicts the resultant load torque for the reference speed pattern depicted in Figure 3. Figure 14 exhibits the speed variations of second order SMC with PIDSS and CSS, SMC and PIC.

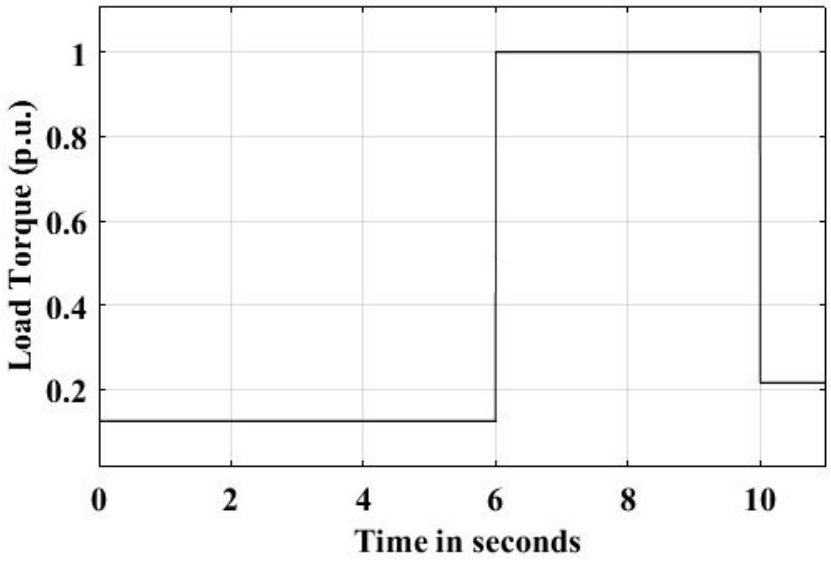

Figure 13 Load Torque - (T_L α ω^3)

The steady state error and peak overshoot exists in the PIC and SMC algorithms. The settling duration of second order CSS is delayed in comparison with second order PIDSS algorithm. The second order PIDSS algorithm is good in tracking the speed without steady state error and peak overshoot. Additionally, second order PIDSS has the fastest speed response time when compared to second order CSS, SMC and PIC.

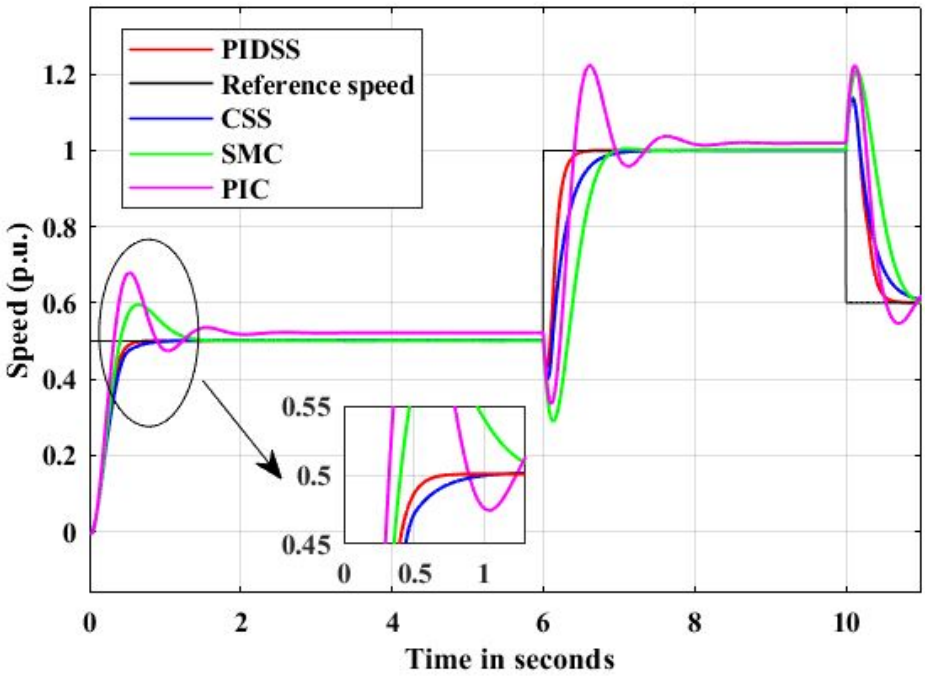

Figure 14 Speed response estimation of PIC, SMC, second order SMC using CSS and PIDSS for the torque due to propeller type load

The previously stated simulation results reveal that for load torque under constant, frictional, fan type and propeller type, second order SMC using PIDSS performs better PIC, SMC and second order SMC with CSS. Table III compares the time that speed settles, peak overshoot and steady state error.

Table III Comparison of PIC, SMC and second order SMC with CSS algorithm and PIDSS algorithm

Time (secs)	Speed reference (p.u.)	Load torque T_L (p.u.)	Speed - settling duration (secs)				Steady-state error %				Peak overshoot%			
			2nd order				2nd order				2nd order			
			PIDSS	CSS	SMC	PIC	PIDSS	CSS	SMC	PIC	PIDSS	CSS	SMC	PIC
	a) load torque under constant circumstances													
0.0 - 4.0	0.5	0	0.587	0.996	1.563	2.111	-	-	12.5	1.6	-	-	-	17.4
4.0 – 6.0	0.5	0.5	0.091	0.492	1.193	1.901	-	-	-	1.8	-	-	-	8
6.0 -8.0	1	0.5	0.496	1.059	1.532	1.907	-	-	6.7	1.2	-	-	-	16
8.0 -10.0	1	1	0.201	0.555	1.156	1.863	-	-	-	-	-	-	-	7.2
10.0 -11.0	0.6	1	0.476	0.996	Not settled	Not settled	-	-	-	-	-	-	-	-
	b) load torque under frictional type circumstances													
0.0 - 6.0	0.5	0.5	0.699	1.014	1.473	2.377	-	-	-	2.3	-	-	4.5	20.7

6.0- 10.0	1	1	0.501	1.101	1.385	2.250	-	-	-	1.8	-	-	1.3	19.3
10.0- 11.0	0.6	0.6	0.583	1.128	Not settled	Not settled	-	-	-	-	-	-	-	-
	c) load torque under fan type circumstances													
0.0 - 6.0	0.5	0.25	0.516	0.791	1.454	2.155	-	-	-	2	-	-	-	19.4
6.0 - 10.0	1	1	0.571	1.130	1.387	2.254	-	-	-	2.1	-	-	-	21.2
10.0- 11.0	0.6	0.36	0.618	1.209	Not settled	Not settled	-	-	-	-	-	-	-	-
	d) load torque under propeller type circumstances													
0.0 - 6.0	0.5	0.125	0.705	1.122	1.433	2.241	-	-	-	2	-	-	9.8	17.8
6.0 - 10.0	1	1	0.524	1.106	1.337	2.246	-	-	-	1.6	-	-	0.9	21.7
10.0- 11.0	0.6	0.216	0.681	1.154	Not settled	Not settled	-	-	-	-	-	-	-	-

Case 5: Robustness under the torque due to undefined type load

In the simulation study, two undefined-load torques (Figure 15 and Figure 17) are chosen to analyze the execution of second order PIDSS. The motor is subjected to the undefined-load torque-1 represented in Figure 15 for the reference speed pattern depicted in Figure 3. Figure 16 portrays the simulation result for the convergence of speed for the torque due to undefined type load pattern-1.

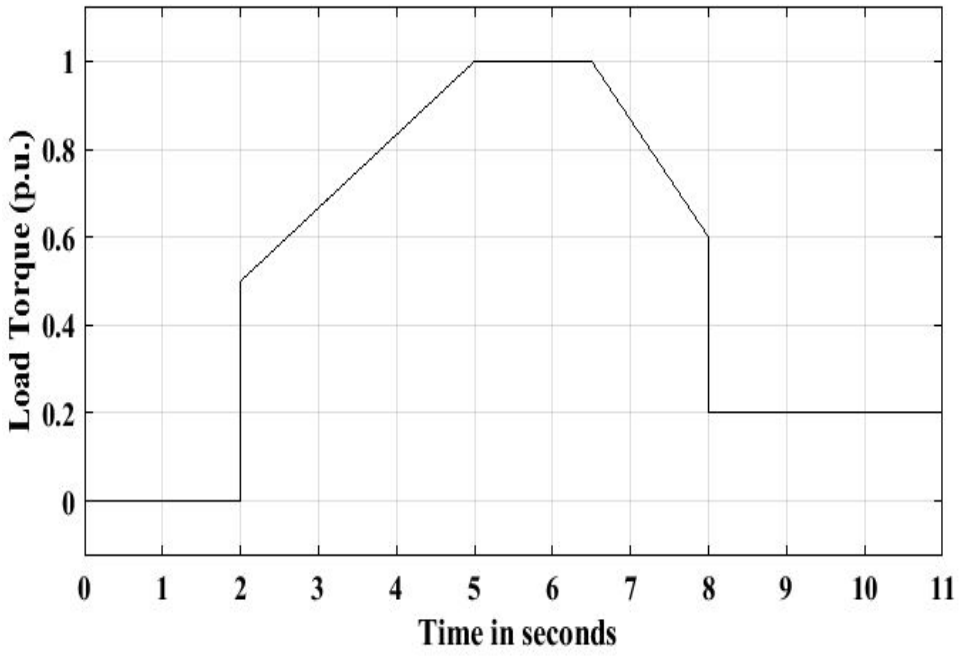

Figure 15 Torque due to undefined type load pattern-1

The correlation among PIC, SMC, second order SMC for the torque due to undefined type load pattern-1 is displayed in Table IV. Second order SMC with PIDSS accumulates the speed quicker than second order SMC with CSS, SMC, and PIC without peak overshoot and steady state error for the torque due to undefined type load pattern-1.

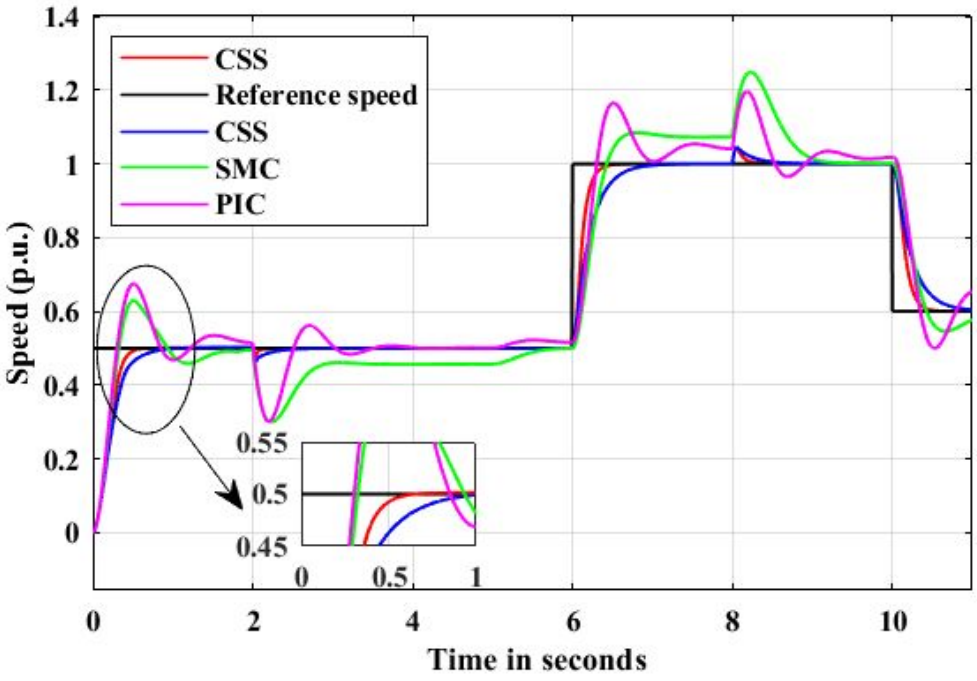

Figure 16 Speed response estimation of PIC, SMC, second order SMC using CSS and PIDSS for the torque due to undefined type load pattern-1

Table IV. Comparative analysis of PIC, SMC and second order SMC using CSS and PIDSS under the torque due to undefined type load pattern-1

Time (secs)	Speed reference changes (p.u.)	Changes in load torque (p.u.) and speed reference (p.u.)	Speed settling time (seconds)			
			2nd order			
			PIDSS	CSS	SMC	PIC
0.0 - 6.0	0.5	i) 0.5 p.u. speed reference at 0 p.u. load torque for 0 to 2 seconds	0.665	0.957	1.671	1.916
		ii) 0.5 p.u. to 1 p.u. of load torque between 2 and 5 seconds of speed reference.	0.098	0.350	1.490	2.168
6.0 - 10.0	1	6 to 10 seconds Load torque varies as 1 p.u. to 0.2 p.u.	0.476	1.004	1.330	1.842
10.0 -11.0	0.6	0.2p.u load torque for the speed reference of 0.6 p.u. from 10 to 11 seconds.	0.547	1.083	Not settled	Not settled

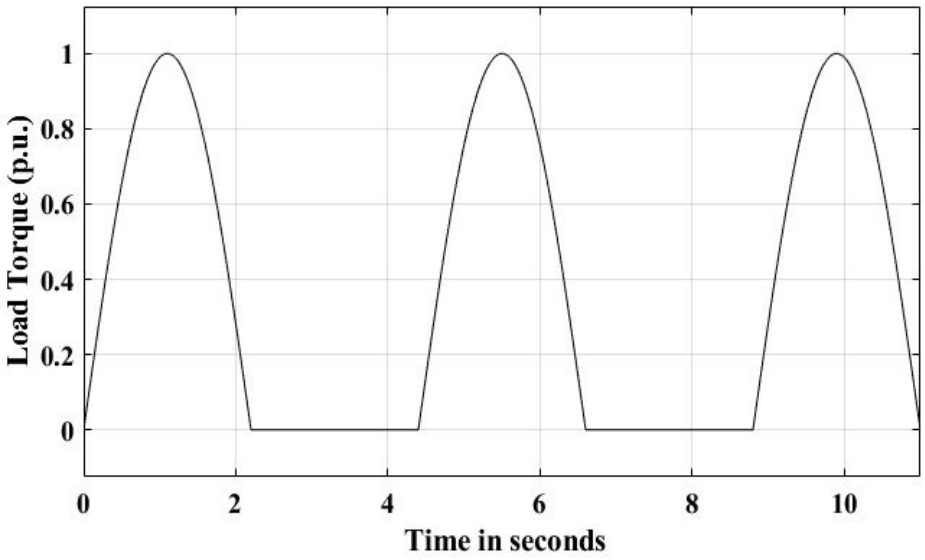

Figure 17 Undefined -load torque-2

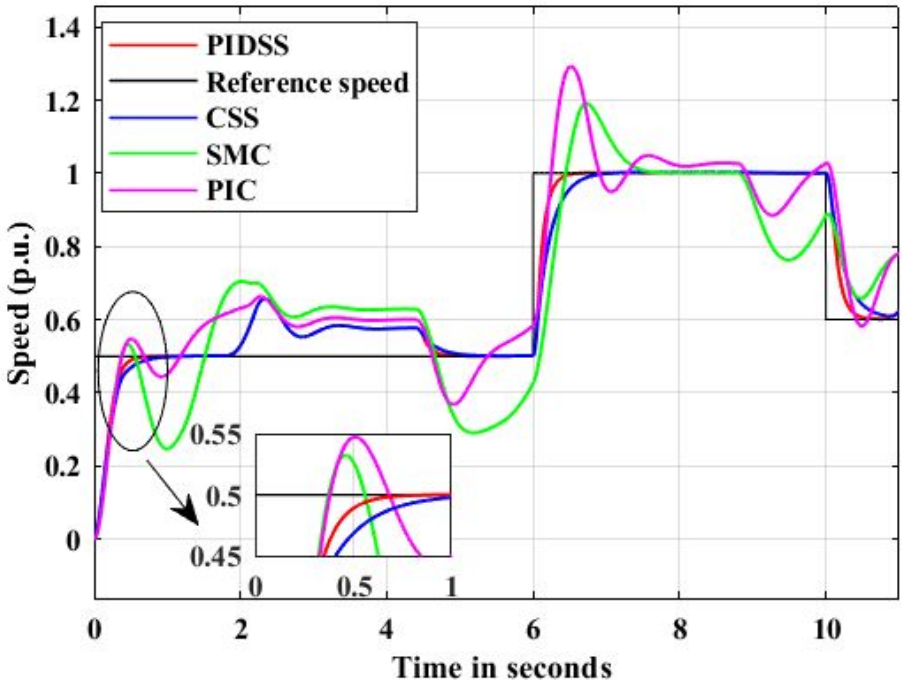

Figure 18 PIC, SMC, second-order SMC using CSS, and PIDSS speed response evaluation for the torque due to undefined type load pattern-2

Figure 17 depicts the torque due to undefined type load pattern-2, which is examined on the PMDC motor for the speed reference pattern depicted in Figure 3. For the torque due to undefined type load pattern-2, the functioning of the CSS with second order, PIDSS with second order, SMC, and PIC are contrasted.

Figure 18 displays the simulation's outcome for the convergence of speed. In Figure 18, it is evident that second-order PIDSS tracks speed accurately without steady-state inaccuracy or peak overshoot.

Table V Comparison of PIC, SMC, second order SMC with CSS and PIDSS the torque due to undefined type load pattern-2

Time (secs)	Speed reference (p.u.)	Settling duration of speed (secs)			
		2nd order			
		PIDSS	CSS	SMC	PIC
0.0 - 6.0	0.5	0.382	0.972	-	-
6.0 - 10.0	1	0.327	0.980	-	-
10.0 - 11.0	0.6	0.406	0.846	-	-

For the torque due to undefined type load pattern-2, the performance evaluation appears in Table V. According to Table V, for speed references of 0.5 p.u, 1 p.u, and 0.6 p.u, second order SMC with PIDSS settles more quickly than second order SMC via CSS, SMC, and PIC.

Case 6: Robustness under the ramp speed variations

In the simulation study, reference ramp speed variations with uniform magnitude and time period are chosen to analyze the execution of second order PIDSS under no load conditions. The reference speed pattern under ramp variations is depicted in Figure 19. In Figure 19, the reference speed changes for every 6 seconds. During the period between 0 seconds to 6 seconds, speed linearly increases from 0 p.u. to 0.5 p.u. and then decreases 0.15 p.u. Thereafter, the speed variation will be between 0.15 p.u. to 0.5 p.u. and then to 0.15 p.u. Figure 20 portrays the simulation result for the convergence of speed under ramp speed variations.

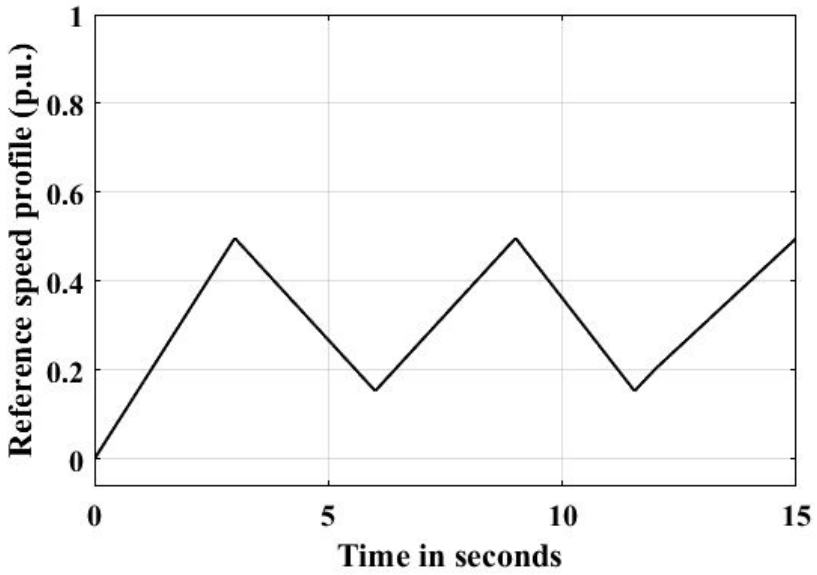

Figure 19 Reference ramp speed pattern

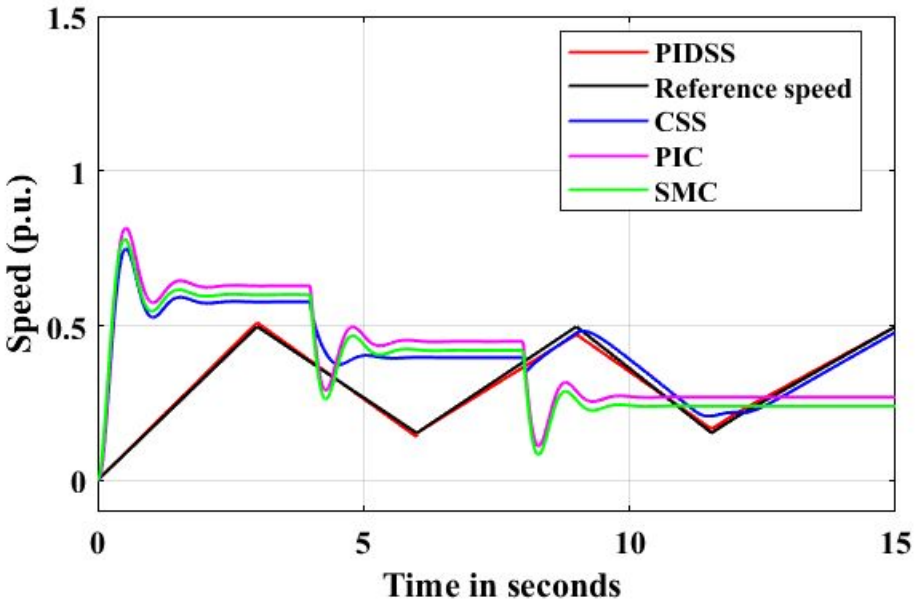

Figure 20 PIC, SMC, second-order SMC using CSS, and PIDSS speed response evaluation for the reference ramp speed pattern

From the Figure 20, the second order PIDSS track the reference ramp speed variations excellently in comparison with second order SMC using CSS, PIC and SMC.

It is clear from the aforementioned simulation study that, second order SMC with PIDSS settles faster than second order SMC using CSS, PIC and SMC for servo tasks and regulatory activities of PMDC motor.

6. EXPERIMENTAL IMPLEMENTATION AND PERFORMANCE DISCUSSIONS

The performance of second order SMC with PIDSS will be evaluated using real-time implementation to verify the simulation results. Figure 21 and Figure 22 depict the real time setup of a PMDC motor powered by boost converter. The framework comprises a 100 MHz digital storage oscilloscope, an input source, a PMDC motor, a power converter circuit, and an FPGA controller. Xilinx is used to program and upload the control algorithms into Spartan-6 XC6SCX9. After uploading is fully completed, the switch 'S' (FGA25N120) in the boost converter is activated by a gate pulse. The sensors in the hardware implementation are equipped with a current sensor (HEO55T01), a voltage sensor (7840 – IC with voltage sensing), and a speed sensor (HEDS5645).

Experimental testing of the motor is performed at an initial speed of 750 rpm, i.e.,50% of the motor rated speed, followed by takeoffs to the rated rpm and descents to 900 rpm, i.e., 60% of the motor rated speed. for constant load torque circumstances. The real-time findings for PIC, SMC, second order SMC with CSS and second order SMC with PIDSS are shown from Figure 23 to Figure 24.

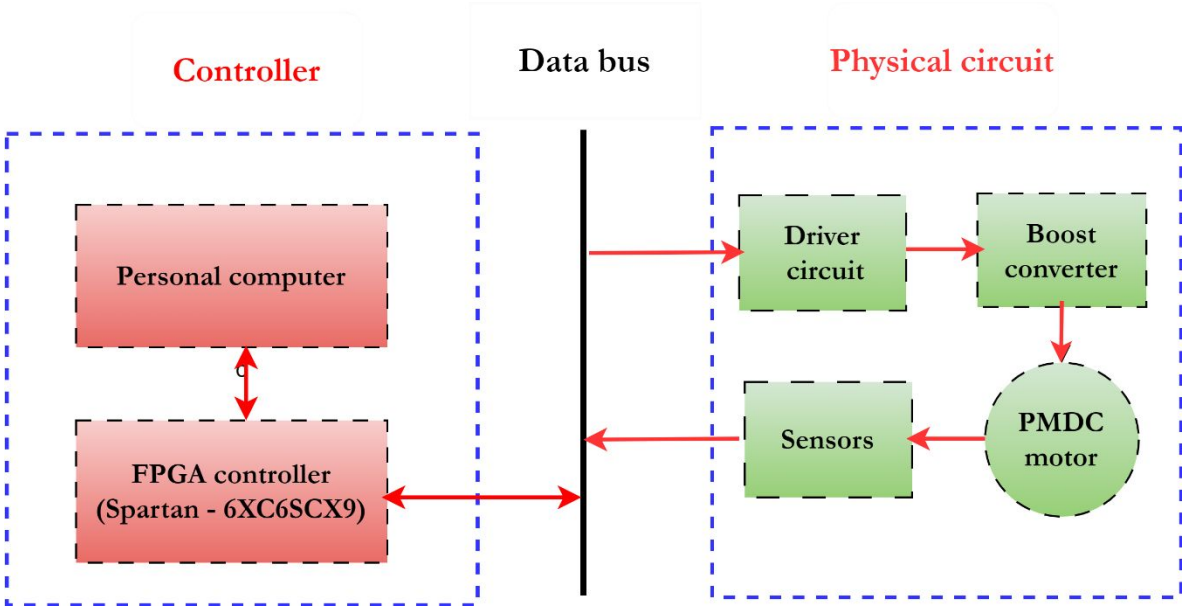

Figure 21 Practical configuration setup

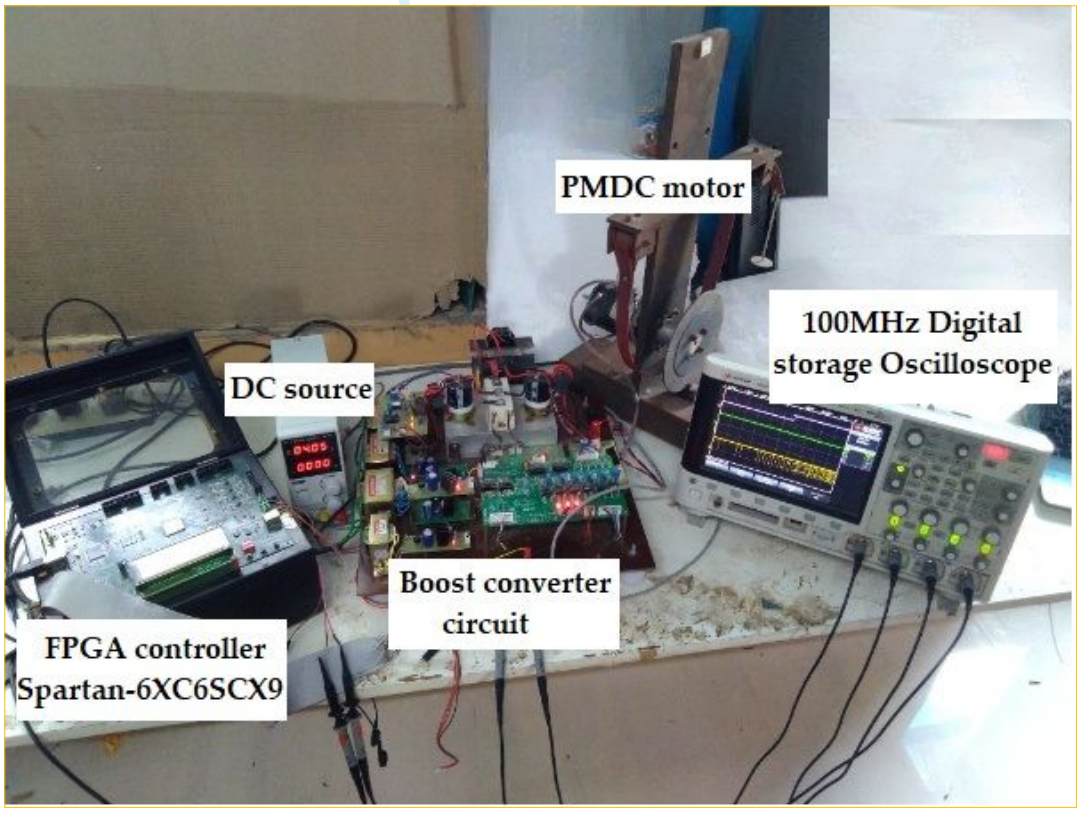

Figure 22 Practical configuration for PMDC motor powered by boost converter

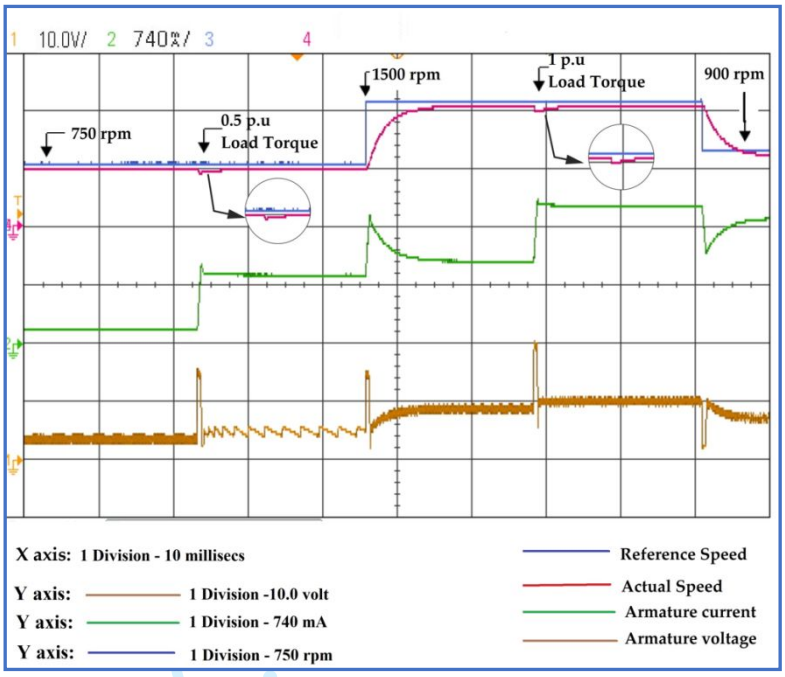

Figure 23 Responses of motor Speed, motor armature current and motor armature voltage changes for second order SMC with CSS

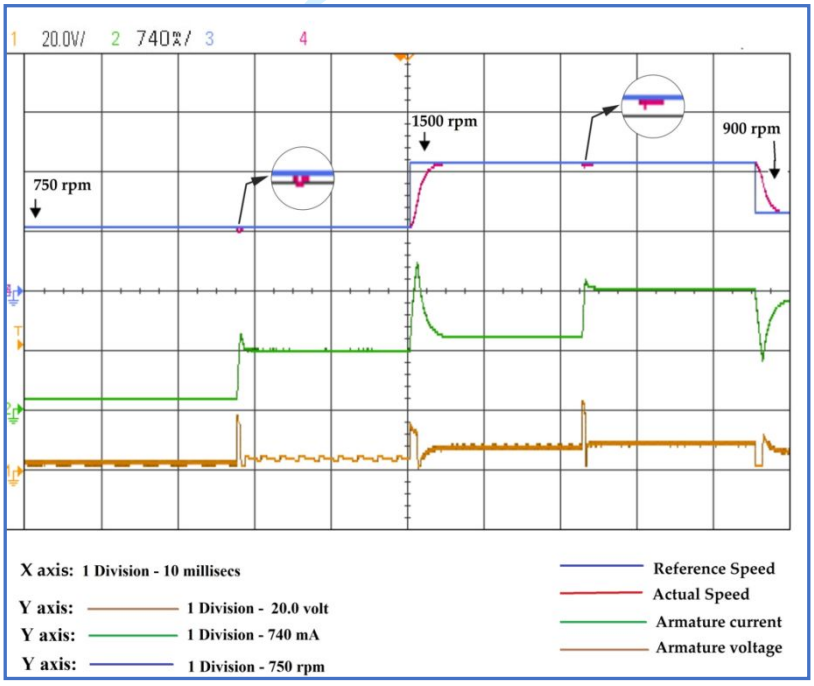

Figure 24 Responses of motor Speed, motor armature current and motor armature voltage changes for second order SMC with PIDSS

The consolidated results for speed, current, and voltage for the second order SMC via CSS are showcased in Figure 23. The consolidated results for speed, current, and voltage for the second order SMC with PIDSS are shown in Figure 24. The results demonstrate that the implementation of second order SMC with CSS does not experience peak overshoot, but the speed tracking is pretty poor in comparison to the reference speed pattern. According to the

findings, second order SMC using PIDSS has a faster settling time than second order SMC using CSS.

Table VI Comparison of second order SMC with CSS and PIDSS in practical configuration for the torque at constant load situation

Variations in Speed reference (rad/sec)	Variations in Speed reference (p.u.)	Load Torque T_L (p.u.)	Settling time of speed (seconds)	
			2nd order	
			PIDSS	CSS
78.5	0.5	0.5 p.u	0.25	0.49
157	1	0.5 p.u	0.35	0.65
157	1	1 p.u	0.3	0.6
94.2	0.6	1 p.u	0.25	0.55

In the experimental set-up, the torque with constant load circumstances, the settling time of both second order SMC via CSS and PIDSS is provided in Table VI. According to Table VI, second order SMC via PIDSS have a good settling time during load torque deviations with fewer chatter and absence of peak over-shoot.

7. CONCLUSION AND FUTURE WORK

According to the present investigations, Sliding Mode Control (SMC), PI control, second order SMC via proportional-integral-derivative sliding surface (PIDSS), and second order SMC via classical-sliding surface (CSS) algorithms are developed and tested for PMDC motor powered by boost converter. Compared to other sliding mode controllers, higher order proportional-integral-derivative sliding surface (PIDSS) are a popular choice for many applications because of their adaptability and broad applicability in a variety of industries and control systems Higher order PIDSS provides continuous and smooth control action, minimizing the possibility of abrupt changes in control output, which is advantageous for systems with delicate or sensitive components. Also, higher order PIDSS suitable for real-time control in environments with limited resources because they typically have low computational requirements.

Through MATLAB, all models are evaluated on a PMDC motor supplied by a boost converter under a variety of load torque conditions, including:

- Constant,
- Frictional,
- Fan type,
- Propeller type and
- Undefined-load.

Using MATLAB simulation, the proposed second order SMC's reliability is examined for,

i) absence of load,
ii) fifty percentage of the load and
iii) maximum loaded circumstances.

Based on the findings of numerical model, it is evident that for deviations in load torque and speed, the behaviour of second order SMC via classical sliding surface, SMC and

PIC is disappointing in terms of obtaining the actual speed, peak over-shoot and error in steady state when compared to second order SMC with PIDSS. The real time results show the effective implementation of the suggested control scheme to control the operating speed of the PMDC motor for constant load torque (at no load, half load, and full load). Consequently, the proposed higher order SMC is capable of servo and regulatory actions for PMDC motors powered by a boost converter. In future, cuk converter and buck-boost converter can be used for implementing the above said control techniques. Further, both low and high-power converters can be used to test the viability of the control method.

ACKNOWLEDGMENT

Authors thank DEEE, College of Engineering Guindy, Anna University, Tamilnadu, India for the financial support through the thematic area "Development of Energy Efficient Motor Drive System for Electric Vehicle" under RUSA 2.0. Also, authors thank the ANID/ ATE220023 Project; FONDECYT Regular Research Project 1220556; CLIMAT AMSUD 21001 and FONDAP SERC Chile 15110019.

References

[1] Ahmad, S. and Ali, A., (2019), "Active disturbance rejection control of DC–DC boost converter: a review with modifications for improved performance", *IET Power Electronics*, Vol.12 No 8, pp.2095-2107.

[2] Alonge, F., D'ippolito, F., Garraffa, G., Giaconia, G.C., Latona, R. and Sferlazza, A., (2023). "Sliding Mode Control of Quadratic Boost Converters Based on Min-Type Control Strategy", *IEEE Access*, Vol.11, pp.39176-39184.

[3] Appikonda, M. and Kaliaperumal, D., (2022), "Design of double-integral sliding-mode controller for fourth-order double input DC - DC boost converter with a voltage multiplier cell", *International Journal of Electronics*, pp.1-22

[4] Asl, A.A., Asl, R.A., Kurdkandi, N.V. and Hosseini, S.H., (2022), "Modelling and controlling A new PV/FC/battery DC–DC converter suitable for DC motor", *The Journal of Engineering*, Vol.6, pp.567-582.

[5] Aydogmus, O., Deniz, E. and Kayisli, K., (2014), "PMSM Drive Fed by Sliding Mode Controlled PFC Boost Converter", *Arabian Journal for Science and Engineering*, Vol.39, No 6, pp.4765-4773.

[6] Babaei, E., Seyed Mahmoodieh, M.E. and Mashinchi Mahery, H., (2012). "Operational Modes and Output-Voltage-Ripple Analysis and Design Considerations of Buck–Boost DC–DC Converters", *IEEE Transactions on Industrial Electronics*, Vol.59, No.1, pp.381-391.

[7] Babaei, E. and Seyed Mahmoodieh, M.E., (2014), "Calculation of Output Voltage Ripple and Design Considerations of SEPIC Converter", *IEEE Transactions on Industrial Electronics*, Vol.6, No.3, pp.1213-1222.

[8] Babaei, E., Abbasnezhad, A., Sabahi, M. and Hosseini, S.H., (2017), "Analysis and design of a soft-switching boost DC/DC converter". *IET Power Electronics*, Vol.10, No.11, pp.1353-1362.

[9] Chincholkar, S.H., Jiang, W. and Chan, C.-Y., (2018), "An Improved PWM-Based Sliding-Mode Controller for a DC–DC Cascade Boost Converter", *IEEE Transactions on Circuits and Systems II: Express Briefs*, Vol.65, No.11, pp.1639-1643.

[10] Corradini, M.L., Ippoliti, G. and Orlando, G., (2022), "Boost converter load estimation by a sliding mode approach", *International Journal of Circuit Theory and Applications*, Vol.50, No.5, pp.1806-1816.

[11] Crescimbini, F., Lidozzi, A., Lo Calzo, G. and Solero, L., (2014). "High-Speed Electric Drive for Exhaust Gas Energy Recovery Applications", *IEEE Transactions on Industrial Electronics*, Vol.61 No 6, pp.2998-3011.

[12] Defoort, M., Floquet, T., Kokosy, A. and Perruquetti, W., (2009). "A novel higher order sliding mode control scheme", *Systems & Control Letters*, Vol.58 No 2, pp.102-108.

[13] Feng, L., Deng, M., Xu, S. and Huang, D., (2020), "Speed Regulation for PMSM Drives Based on a Novel Sliding Mode Controller", *IEEE Access*, Vol.8, pp.63577-63584.

[14] Inomoto, R.S., Monteiro, J.R.B. de A. and Filho, A.J.S., (2022). "Boost Converter Control of PV System Using Sliding Mode Control With Integrative Sliding Surface", *IEEE Journal of Emerging and Selected Topics in Power Electronics*, Vol.10, No.5, pp.5522-5530.

[15] Kumar, K.R. and Jeevananthan, S., (2012), "Analysis, Design, and Implementation of Hysteresis Modulation Sliding-mode Controller for Negative-output Elementary Boost Converter", *Electric Power Components and Systems*, Vol.40, No.3, pp.292-311.

[16] Komurcugil,H, Biricik,S, Bayhan,S and Zhang, Z (2021), "Sliding Mode Control: Overview of Its Applications in Power Converters," *in IEEE Industrial Electronics Magazine*, Vol. 15, No. 1, pp. 40-49.

[17] Levant, A., (2005), "Homogeneity approach to high-order sliding mode design", *Automatica*, Vol.41, No.5, pp.823-830.

[18] Li, Z., Chen, J., Gan, M. and Zhang, G., (2011). "Adaptive robust control for DC motors with input saturation", *IET Control Theory & Applications*, Vol.5 No.16, pp.1895-1905.

[19] Mahafzah, K.A., Al-Shetwi, A.Q., Hannan, M.A., Babu, T.S. and Nwulu, N., (2023). "A New Cuk-Based DC-DC Converter with Improved Efficiency and Lower Rated Voltage of Coupling Capacitor", *Sustainability*, Vol.15, No.11, pp.8515.

[20] Malge, S.V., Ghogare, M.G., Patil, S.L., Deshpande, A.S. and Pandey, S.K., (2023). "Chatter-Free Non-Singular Fast Terminal Sliding Mode Control of Interleaved Boost Converter", *IEEE Transactions on Circuits and Systems II: Express Briefs*, Vol.70, No 1, pp.186-190.

[21] Mishra, P., Banerjee, A., Ghosh, M. and Baladhandautham, C.B., (2021), "Digital pulse width modulation sampling effect embodied steady-state time-domain modeling of a boost converter driven permanent magnet DC brushed motor", *International Transactions on Electrical Energy Systems*, Vol.31 No 8.

[22] Nizami, T.K., Chakravarty, A., Mahanta, C., Iqbal, A. and Hosseinpour, A., (2022). "Enhanced dynamic performance in DC–DC converter-PMDC motor combination through an intelligent non-linear adaptive control scheme",. *IET Power Electronics*, Vol,15 No.15, pp.1607-1616.

[23] Oucheriah, S., (20140, "PWM-based adaptive sliding mode control for the boost converter with unknown parameters", *International Journal of Electronics Letters*, Vol.2, No 2, pp.92-99.

[24] Pandey, O.H., Shubham,, Sharma, V., Shekhar, S., A, A. and Govindharaj, A., (2021), "Design & Analysis of Sliding Mode Controller for Fuel Cell based DC-DC Boost Converter fed by PMDC Motor", *2021 Asian Conference on Innovation in Technology (ASIANCON)*.

[25] Pisano, A., Davila, A., Fridman, L. and Usai, E., (2008), "Cascade control of PM-DC drives via second-order sliding mode technique", *2008 International Workshop on Variable Structure Systems*.

[26] Rauf, A., Zafran, M., Khan, A. and Tariq, A.R., (2021). "Finite-time nonsingular terminal sliding mode control of converter-driven DC motor system subject to unmatched disturbances", *International Transactions on Electrical Energy Systems*, Vol.31 No11.

[27] Ravikumar, D. and Srinivasan, G.K., (2022), "Implementation of higher order sliding mode control of DC–DC buck converter fed permanent magnet DC motor with improved performance" *Automatika*, Vol.64, No.1, pp.162-177.

[28] Rivera, J., Ortega-Cisneros, S., Rosas-Caro, J.C. and Ruíz-Martínez, O.-F., (2023), "Sliding Mode Regulation of a Boost Circuit for DC-Biased Sinusoidal Power Conversion", *Applied Sciences*, Vol 13, No 10, pp.5963.

[29] Sha, D., Zhang, J., Wang, X. and Yuan, W., (2017). "Dynamic Response Improvements of Parallel-Connected Bidirectional DC–DC Converters for Electrical Drive Powered by Low-Voltage Battery Employing Optimized Feedforward Control", *IEEE Transactions on Power Electronics*, Vol.32 No 10, pp.7783-7794.

[30] Spurgeon, S., (2014), Sliding mode control: a tutorial. *2014 European Control Conference (ECC)*.

[31] Tan, S.-C., Lai, Y.-M. and Tse, C.-K., (2018), *Sliding Mode Control of Switching Power Converters*. CRC Press.

[32] Utkin, V., (1993). "Sliding mode control design principles and applications to electric drives", *IEEE Transactions on Industrial Electronics*, Vol.40 No.1, pp.23-36.

[33] Waghmare, T.T. and Chaturvedi, P., (2023), "Super twisting approach of a higher order sliding mode controller for a flyback DC–DC converter in photovoltaic applications", *International Journal of Circuit Theory and Applications*, pp.1-18.

[34] Wai, R.-J. and Shih, L.-C., (2011), "Design of Voltage Tracking Control for DC–DC Boost Converter Via Total Sliding-Mode Technique", *IEEE Transactions on Industrial Electronics*, Vol.58 No.6, pp.2502-2511.

[35] Wu, J. and Lu, Y., (2019), "Adaptive Backstepping Sliding Mode Control for Boost Converter With Constant Power Load", *IEEE Access*, Vol.7, pp.50797-50807.

[36] Yang, J., Wu, H., Hu, L. and Li, S., (2019). "Robust Predictive Speed Regulation of Converter-Driven DC Motors via a Discrete-Time Reduced-Order GPIO", *IEEE Transactions on Industrial Electronics*, Vol.66, No.10, pp.7893-7903.

[37] Zambrano-Prada, D.A., El Aroudi, A., Vazquez-Seisdedos, L. and Martinez-Salamero, L., (2023), "Polynomial Sliding Surfaces to Control a Boost Converter With Constant Power Load", *IEEE Transactions on Circuits and Systems I: Regular Papers*, Vol.70, No 1, pp.530-543.

REVIEWER COMMENTS AND REPLIES

Manuscript ID: CW-06-2023-0144.R1

Manuscript Title: A novel higher-order sliding mode control for DC-DC boost converter system in PMDC motor exploring mismatched disturbances

Journal: Circuit World

Esteemed Editor and Reviewers,

We would like to express our thanks to Editor –in-Chief, Associate Editor, Assistant Editor and reviewers for recommending our article with major revisions. Further, it is informed that based on all the comments suggested **(R1)**, authors modified the paper completely for further consideration. The following are the point-to-point responses to the comments. Revisions **(R1)** are highlighted in yellow colour. Thank you very much in advance for taking your time in reviewing this revised manuscript.

Reviewer #1

Recommendation: Minor Revision

Esteemed Editor and Reviewers,

First of all, we would like to take this opportunity to express our sincere thanks to the reviewers for giving **minor revision**. All the suggestions are updated in the manuscript and revisions are highlighted in yellow colour. In the following, a point-by-point reply to the reviewers' comment are presented:

Reviewer #1: Query 1:

Please improve the quality of the waveforms (Fig. 19 & 20), incl. the scales of x/y axes and the original points.

[Authors' reply]

Authors thank the honourable reviewers for the valuable comment. Now the resolution of Figures is improved and the scales of the waveforms (Fig. 19 & 20) are labeled clearly. The changes are updated in the revised manuscript.

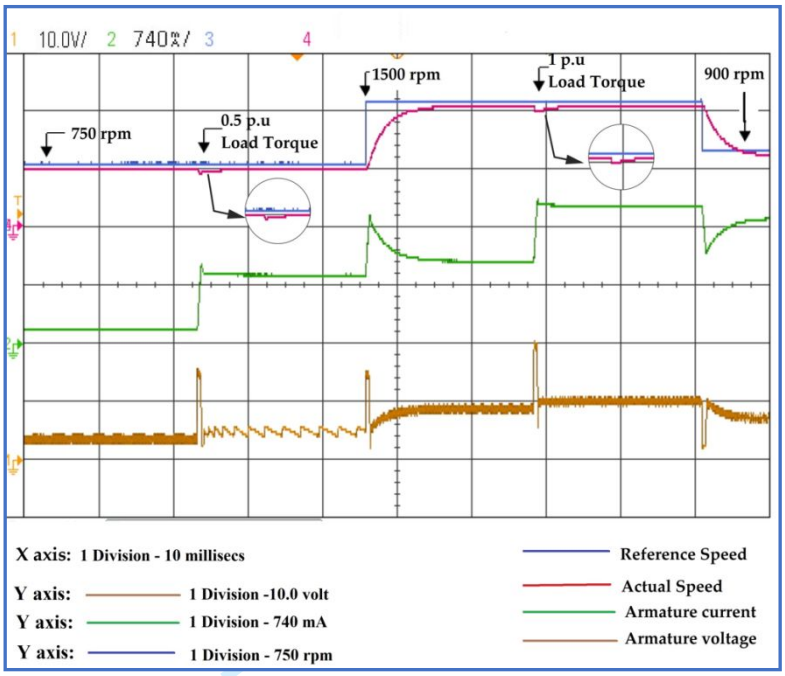

Figure 23 Responses of motor Speed, motor armature current and motor armature voltage changes for second order SMC with CSS

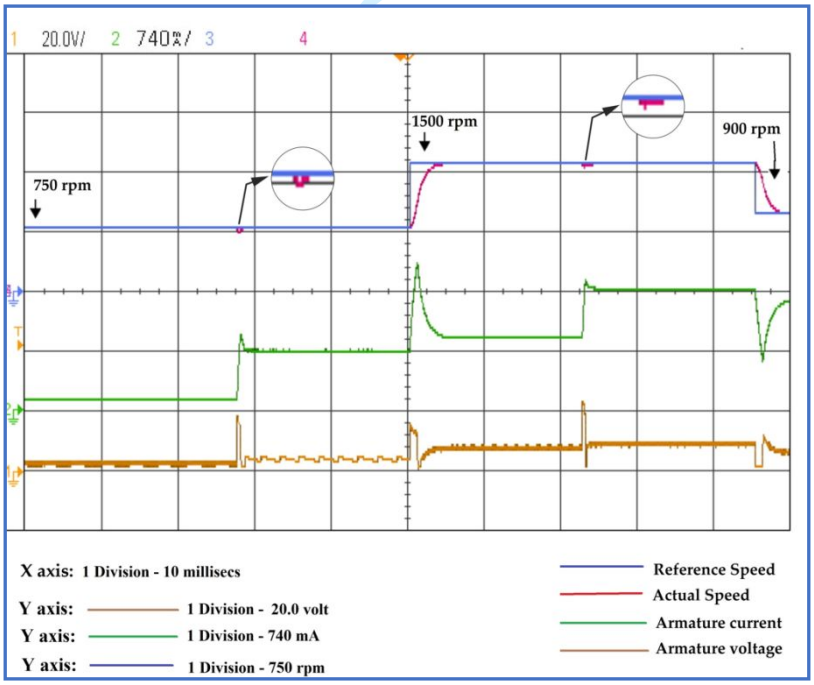

Figure 24 Responses of motor Speed, motor armature current and motor armature voltage changes for second order SMC with PIDSS

Reviewer #1: Query 2:

In terms of my Question 4, please note that the rotational speed of motors should not normally have a sudden change. The testing conditions are thereby supposed to be modified.

[Authors' reply]

Thanks for the comment. In Revision 1, Question 4, honourable reviewers recommended to validate the methodologies under more mild speed variation (e.g., ramp change). Authors simulated for ramp change variations with various magnitude and time period. The results with discussions are updated in the revised manuscript (Revision 1). Furthermore, in Revision 2, authors have modified the testing conditions to reflect mild speed variations, specifically ramp changes, with uniform magnitudes and time periods. These updated results are now included in the revised manuscript (Revision 2).

Case 6: Robustness under the ramp speed variations

In the simulation study, reference ramp speed variations with uniform magnitude and time period are chosen to analyze the execution of second order PIDSS under no load conditions. The reference speed pattern under ramp variations is depicted in Figure 19. In Figure 19, the reference speed changes for every 6 seconds. During the period between 0 seconds to 6 seconds, speed linearly increases from 0 p.u. to 0.5 p.u. and then decreases 0.15 p.u. Thereafter, the speed variation will be between 0.15 p.u. to 0.5 p.u. and then to 0.15 p.u. Figure 20 portrays the simulation result for the convergence of speed under ramp speed variations.

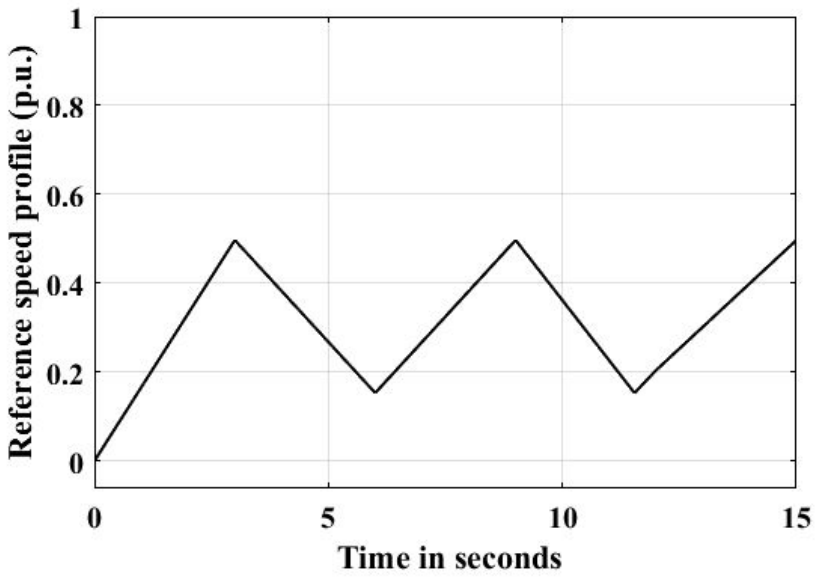

Figure 19 Reference ramp speed pattern

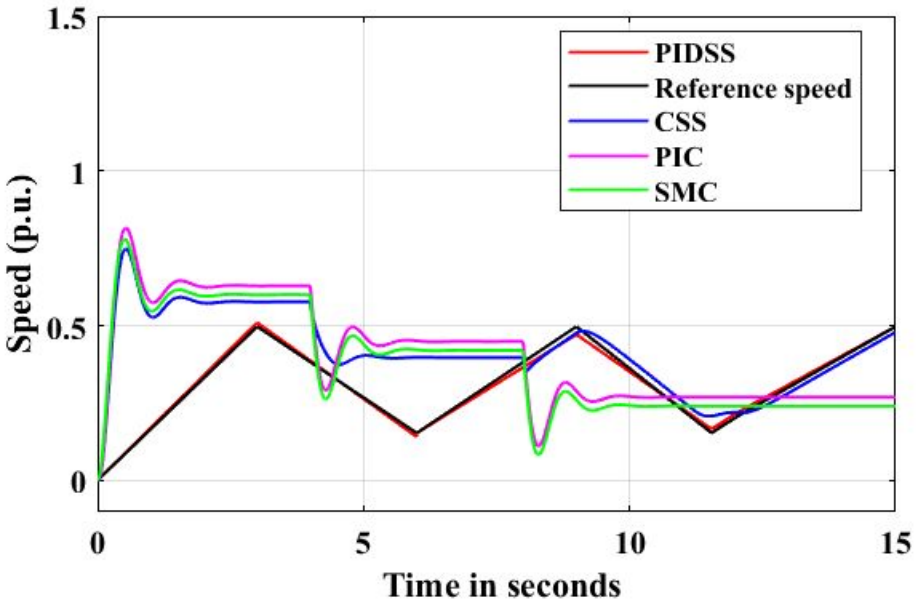

Figure 20 PIC, SMC, second-order SMC using CSS, and PIDSS speed response evaluation for the reference ramp speed pattern

From the Figure 20, the second order PIDSS track the reference ramp speed variations excellently in comparison with second order SMC using CSS, PIC and SMC.

Reviewer #1: Query 3:

Please incorporate your answer to my Question 5 (the constant terms) to your manuscript. All constant terms in your method should be defined clearly.

[Authors' reply]

Now the authors incorporated the answer to the question 5 in the manuscript which is highlighted in yellow colour and the constant terms are defined clearly. Thanks to the reviewers.

Reviewer #2

Recommendation: Accept

Esteemed Reviewer,

First of all, we would like to take this opportunity to express our sincere thanks to the reviewer for **accepting our manuscript** for publication.

Reviewer #2: Query 1:

English still has to be revised to overcome some grammatical errors in the text.

[Authors' reply]

Authors thank the honourable reviewer for the valuable comment. Authors improved the way of writing and corrected the grammatical mistakes in the revised manuscript.

Reviewer #4

Recommendation: Minor Revision

Reviewer #4: Query 1:

No results have been given about the inductor current of the converter and its switch voltage, it is suggested to give at least some explanations about them and add experimental results if possible.

[Authors' reply]

Authors thank the honourable reviewers for the valuable comment. In the manuscript authors proposed the second order PIDSS for boost converter fed PMDC motor and shown the experimental results for constant load torque. As per the comment received from the honourable reviewers, authors incorporated the simulation results for inductor current and armature voltage of the converter for constant load torque conditions in the revised manuscript. Due to time constraints and limitations in laboratory resources, only simulation results have been presented. However, the authors intend to include the suggested experimental results for a four-quadrant converter with higher-order sliding mode control in future research endeavours.

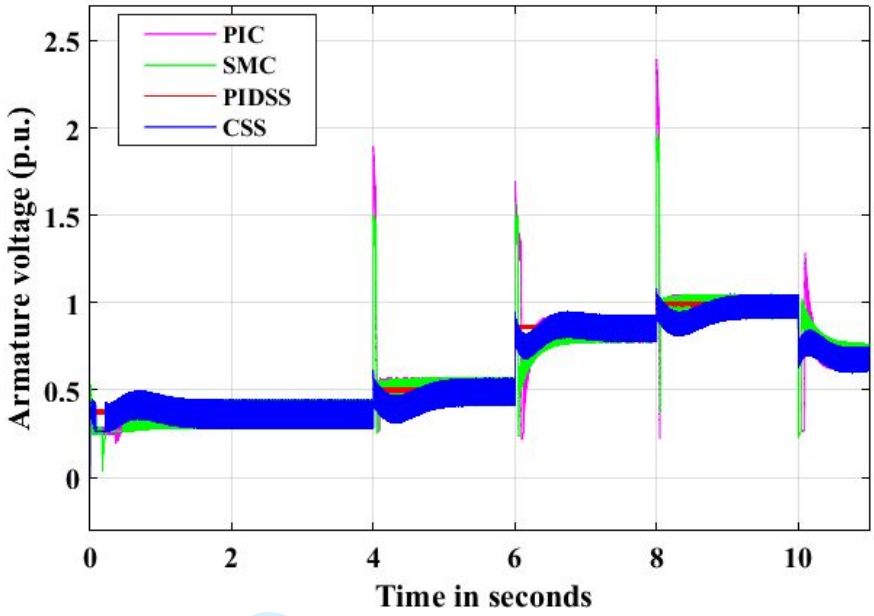

Figure 7 Inspection of the armature voltage response of PIC, SMC, second-order SMC with CSS and PIDSS for the torque at constant load

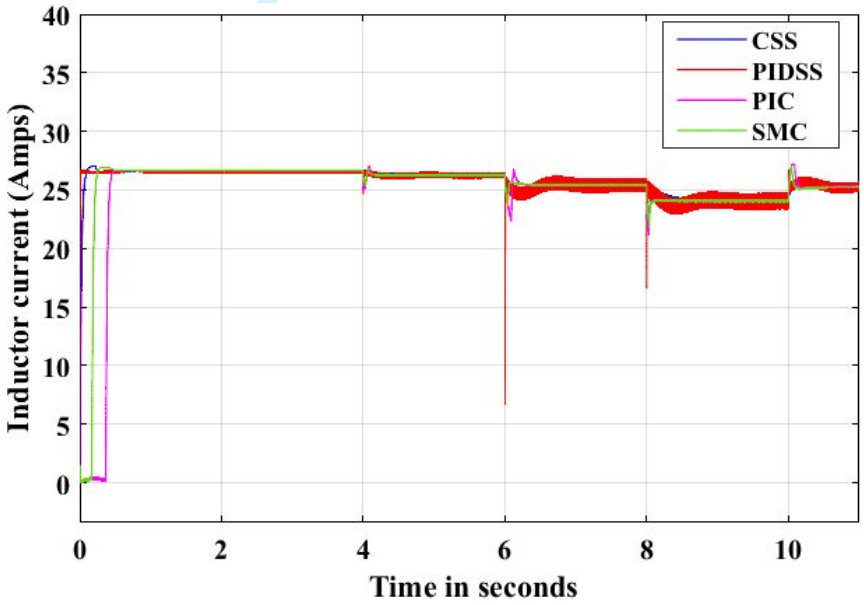

Figure 8 Inspection of the inductor current response of PIC, SMC, second-order SMC with CSS and PIDSS for the torque at constant load

Figures 7 and 8 illustrate the armature voltage and inductor current responses of the boost converter under constant load torque conditions. The response of both armature voltage and inductor current exhibits a smoother behaviour when employing second-order SMC with PIDSS, as compared to PIC, SMC, and second-order SMC with CSS.

Reviewer #4: Query 2:

The number of tables is large, which is a bit confusing. Adding a table with a smaller number and better organization is recommended to make the paper easier to read.

[Authors' reply]

Thanks for your feedback and suggestions. Now the number of Tables are reduced and the following Tables are used,

Table I. Survey of SMC relating to various applications with challenges addressed

Table II. Specifications of boost converter with PMDC motor and the machine behaviour

Table III. Comparison of PIC, SMC and second order SMC with CSS algorithm and PIDSS algorithm

Table IV. Comparative analysis of PIC, SMC and second order SMC using CSS and PIDSS under the torque due to undefined type load pattern-1

Table V. Comparison of PIC, SMC, second order SMC with CSS and PIDSS the torque due to undefined type load pattern-2

Table VI. Comparison of second order SMC with CSS and PIDSS in practical configuration for the torque at constant load situation

---

Reviewer #4: Query 3:

The results of the simulations have been shown in detail for different controllers when applying constant, step, and pseudo-sine loads. Still, the experimental results, which are very valuable, have been done only for no load and constant load. If possible, tests should be done for other methods and loads.

[Authors' reply]

Authors thank the honourable reviewers for the valuable comment. Authors did the simulation work for constant, step, and pseudo-sine loads. The experimental results for no load and constant load situations have been shown in the manuscript. For the remaining load torques authors need another motor with the same rating (To couple both of them) to obtain the experimental results. Due to the limitations in the laboratory set up and time, authors planned to incorporate the suggestions given by honourable reviewers in future. Thanks.

Reviewer #4: Query 4:

Why is the sinusoidal load torque only checked at the positive peak? It is also suggested to give more explanations about the reason for the big difference between conventional methods and the proposed method.

[Authors' reply]

Authors thank the honourable reviewers for the valuable comment. The positive peak of a sinusoidal waveform typically represents the point of highest torque demand on the system. The negative sinusoidal load torque creates the flow of negative current and also it allows regeneration which flows the power towards the source. In the manuscript, authors implemented boost converter which is operated in unidirectional mode. So only authors

suggested positive sinusoidal load torque. In future, authors planned to implement the proposed higher order sliding mode control for four quadrant converter to analyse the sinusoidal load torque both in positive and negative peak. Thanks.

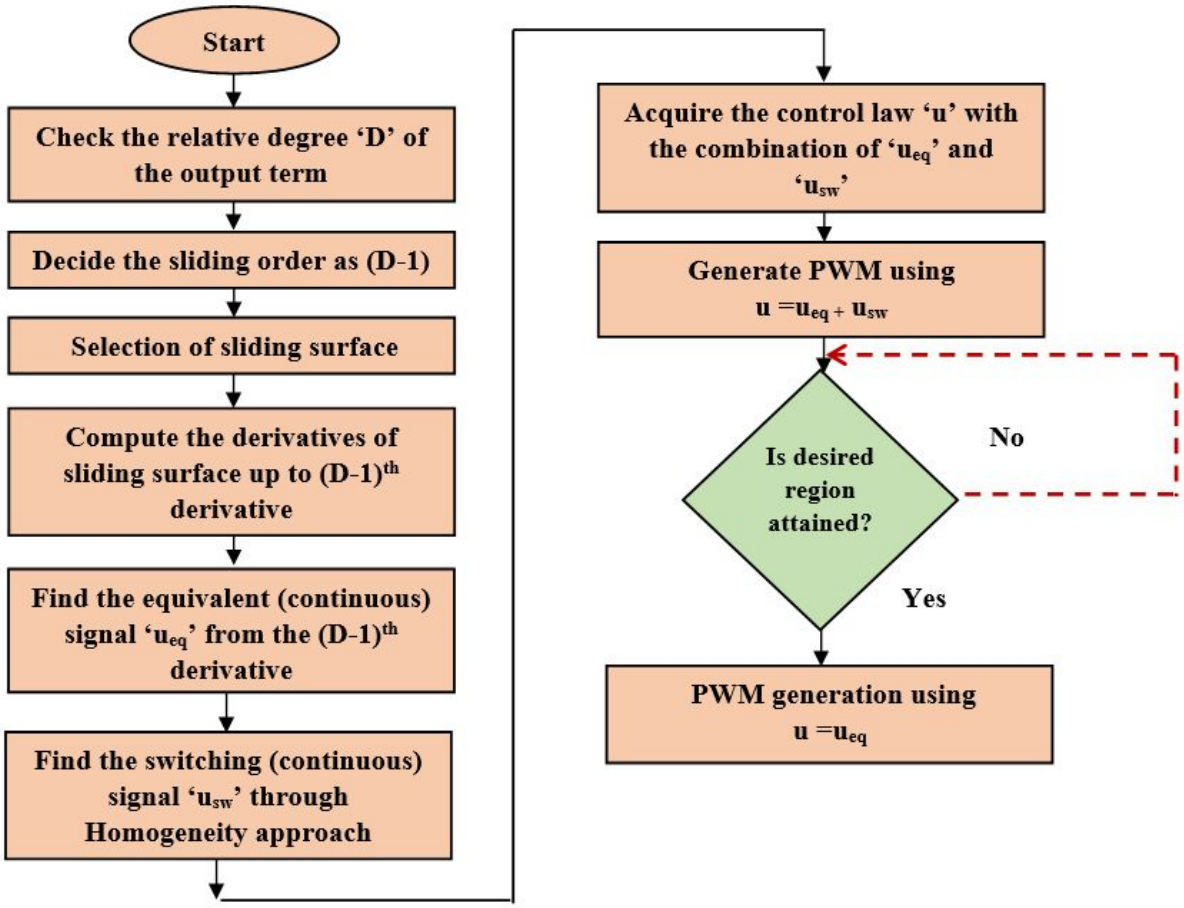

Figure 1 Flowchart representation of HOSMC design

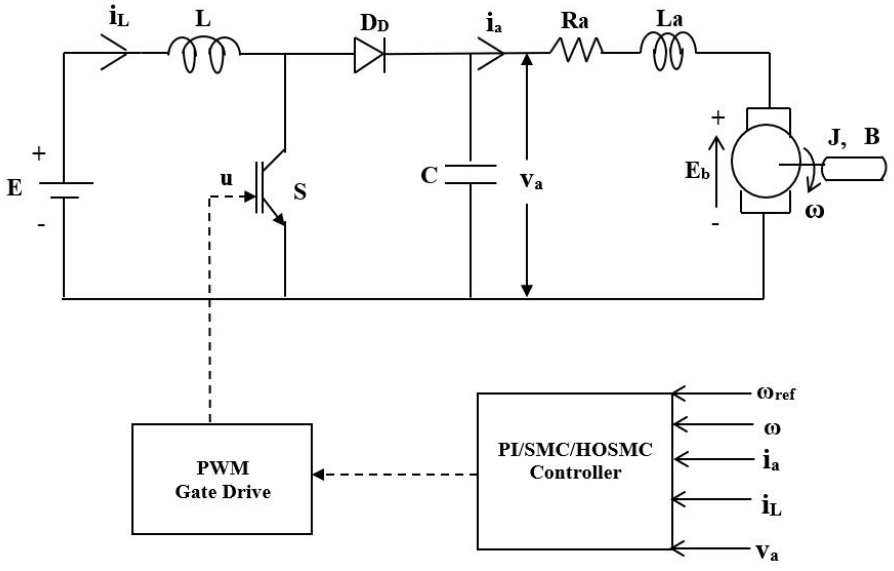

Figure 2 Diagram for PMDC motor powered by boost converter

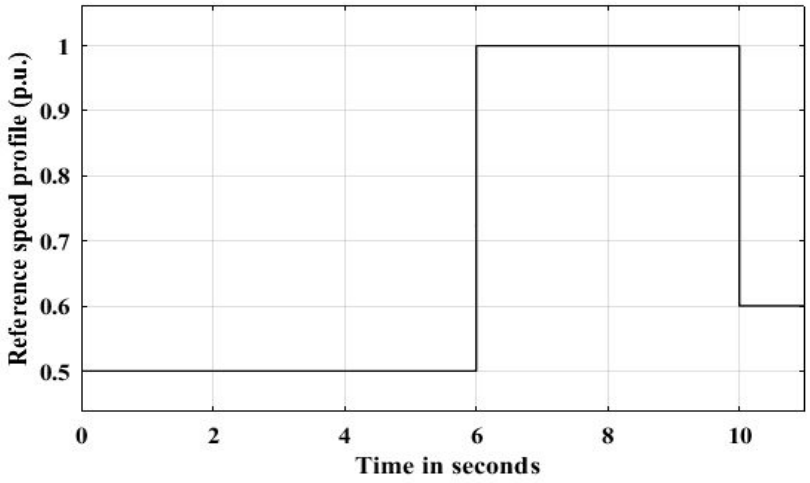

Figure 3 Speed reference pattern

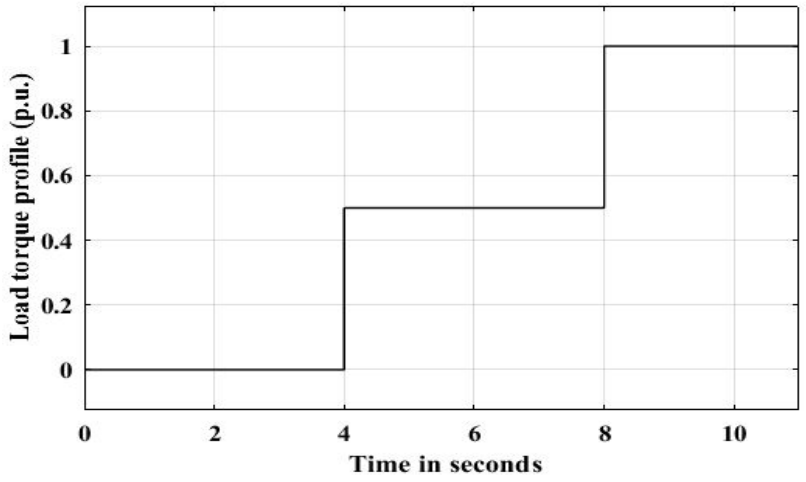

Figure 4 Load torque pattern

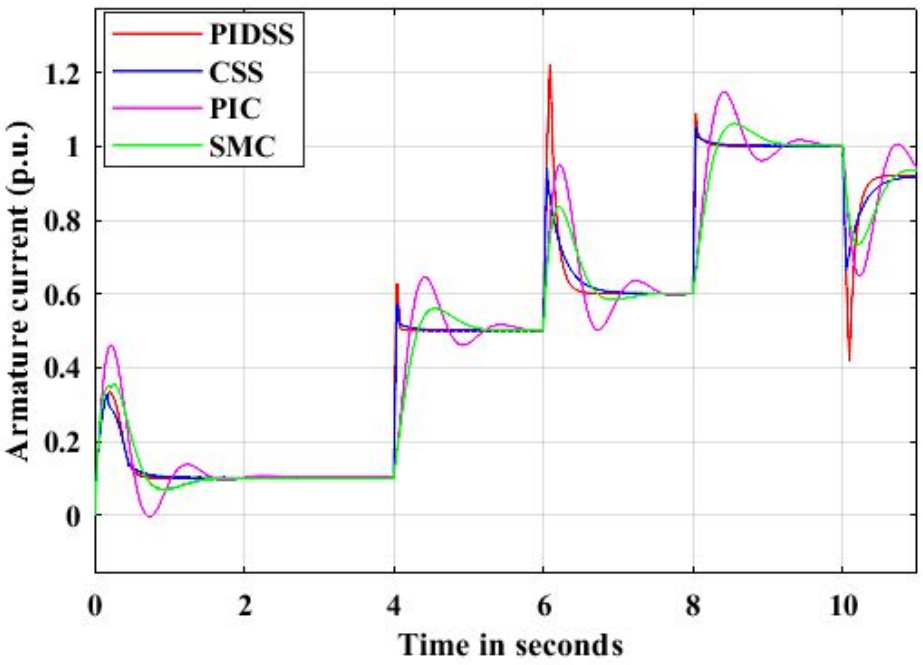

Figure 5 Comparison of armature current between PIC, SMC, second order SMC using CSS and PIDSS for the torque at constant load

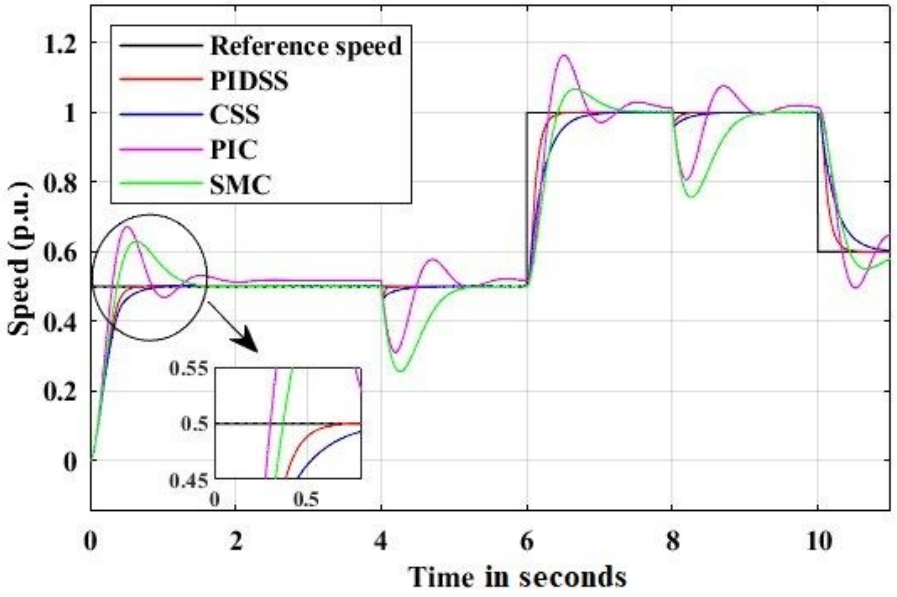

Figure 6 Inspection of the speed response of PIC, SMC, second-order SMC with CSS and PIDSS for the torque at constant load

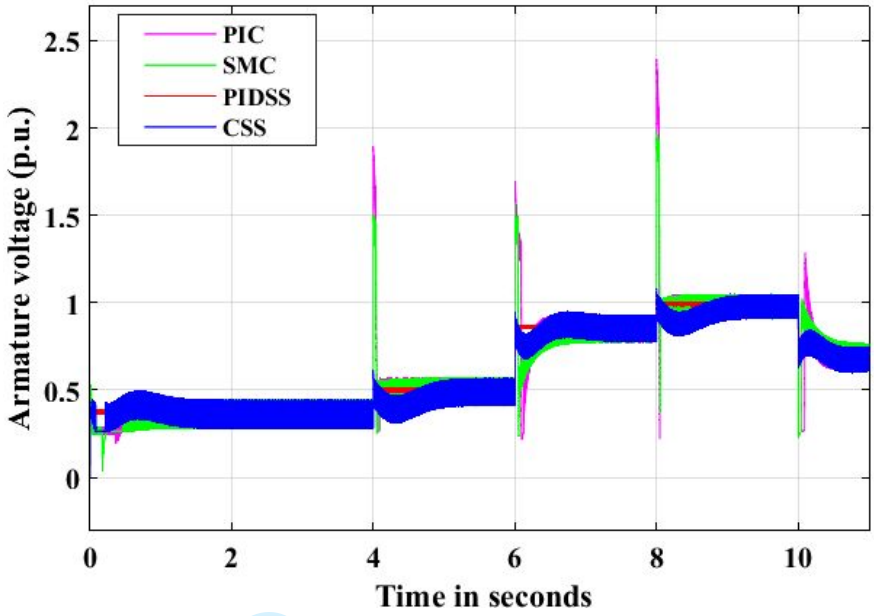

Figure 7 Inspection of the armature voltage response of PIC, SMC, second-order SMC with CSS and PIDSS for the torque at constant load

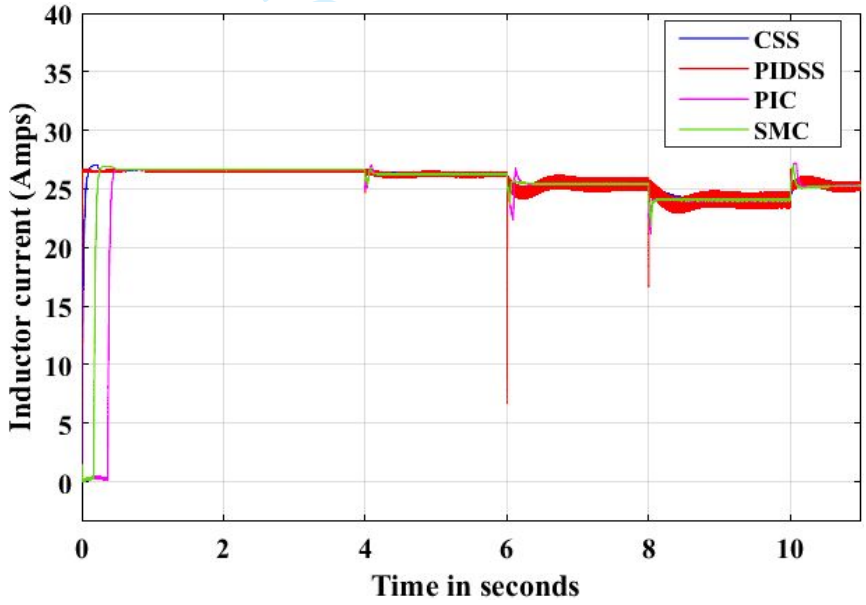

Figure 8 Inspection of the inductor current response of PIC, SMC, second-order SMC with CSS and PIDSS for the torque at constant load

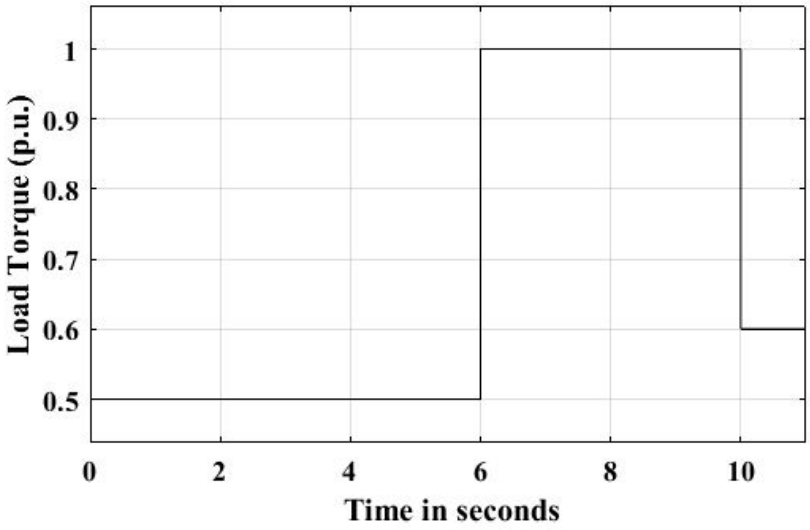

Figure 9 Torque due to frictional load - (T_L α ω)

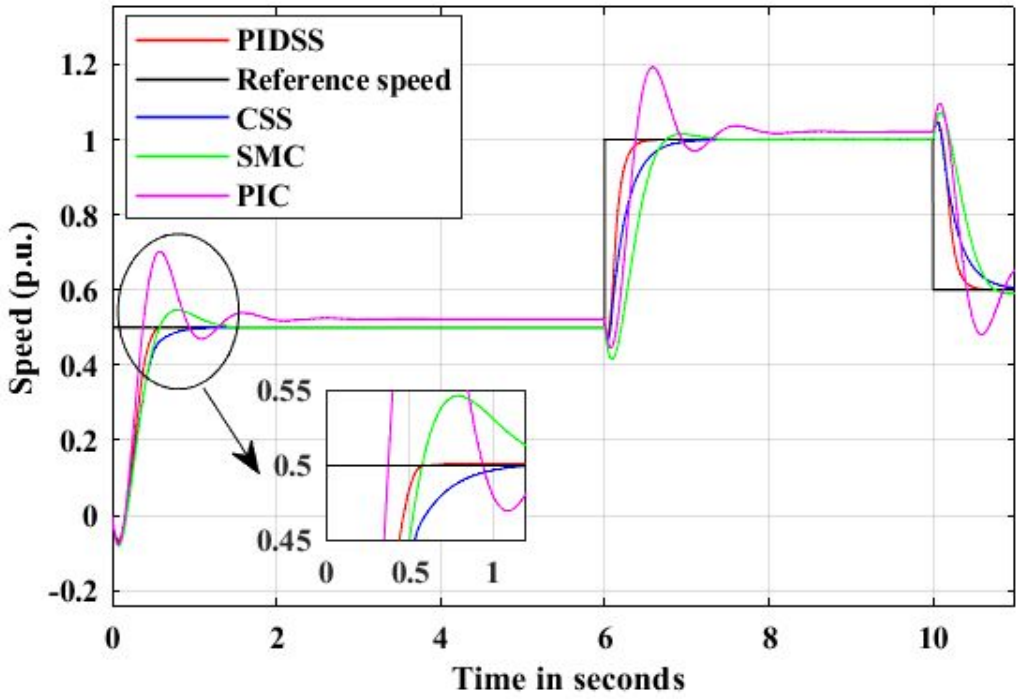

Figure 10 Speed response comparative study between PIC, SMC, second order SMC using CSS and PIDSS over frictional load torque

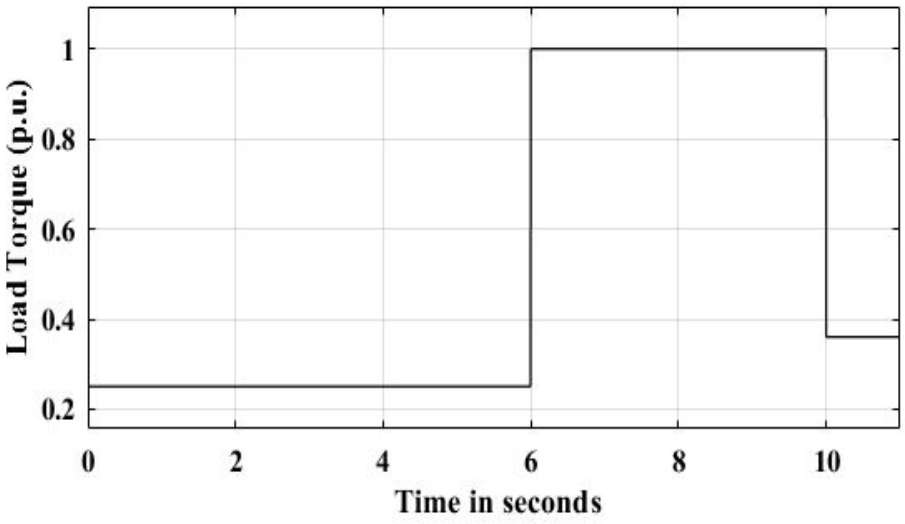

Figure 11 Torque due to fan type load - (T_L α ω^2)

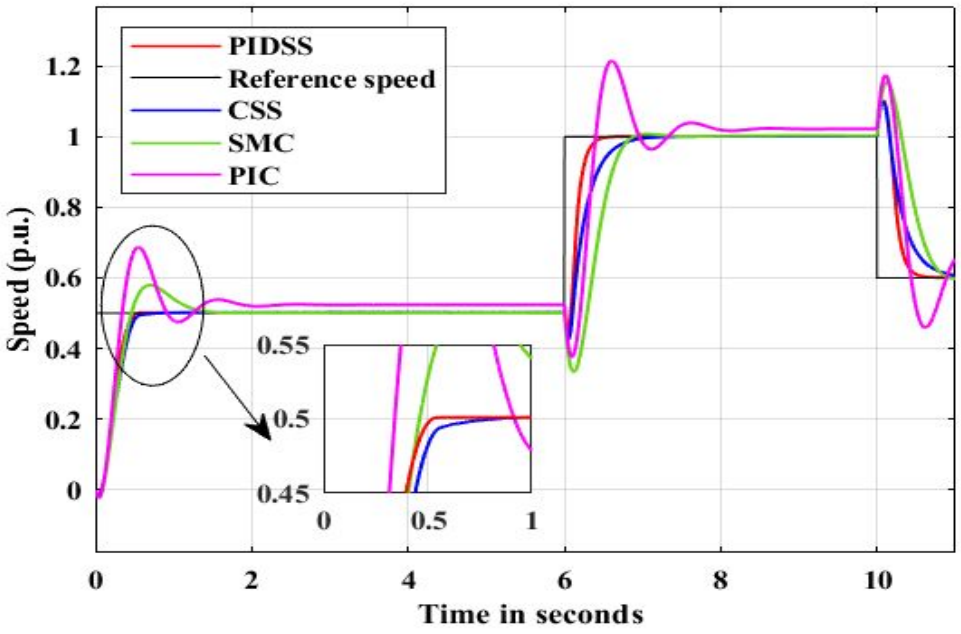

Figure 12 Speed response correlation between PIC, SMC, second order SMC using CSS and PIDSS for the torque due to fan type load

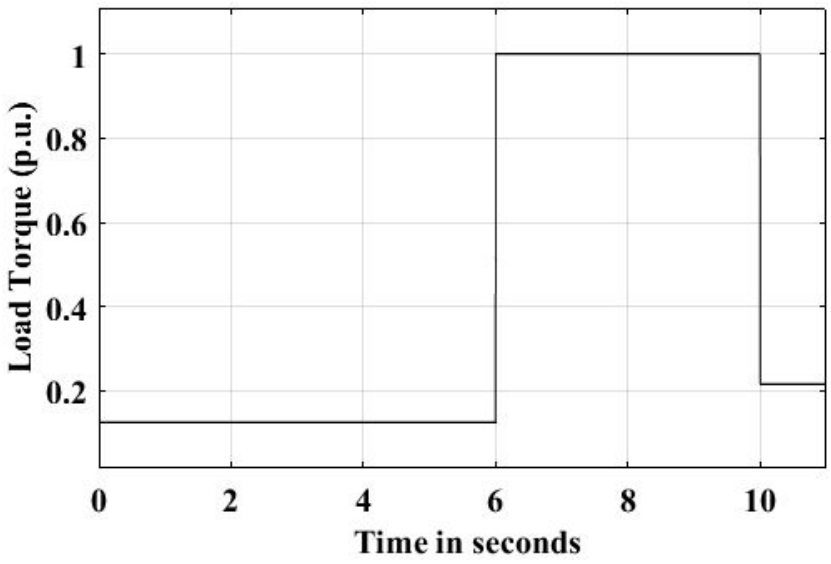

Figure 13 Load Torque - (T_L α ω^3)

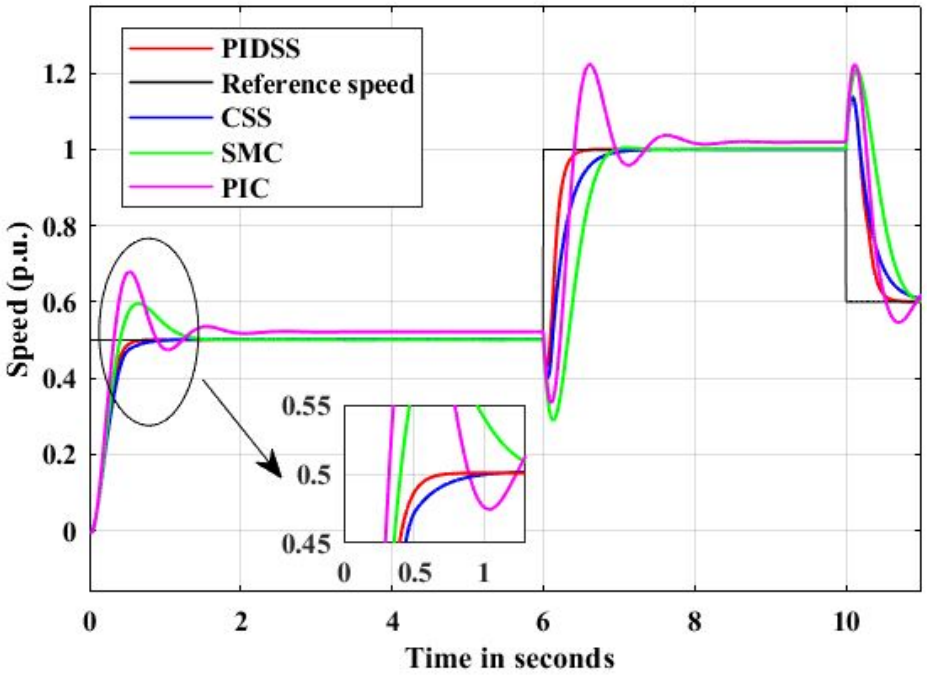

Figure 14 Speed response estimation of PIC, SMC, second order SMC using CSS and PIDSS for the torque due to propeller type load

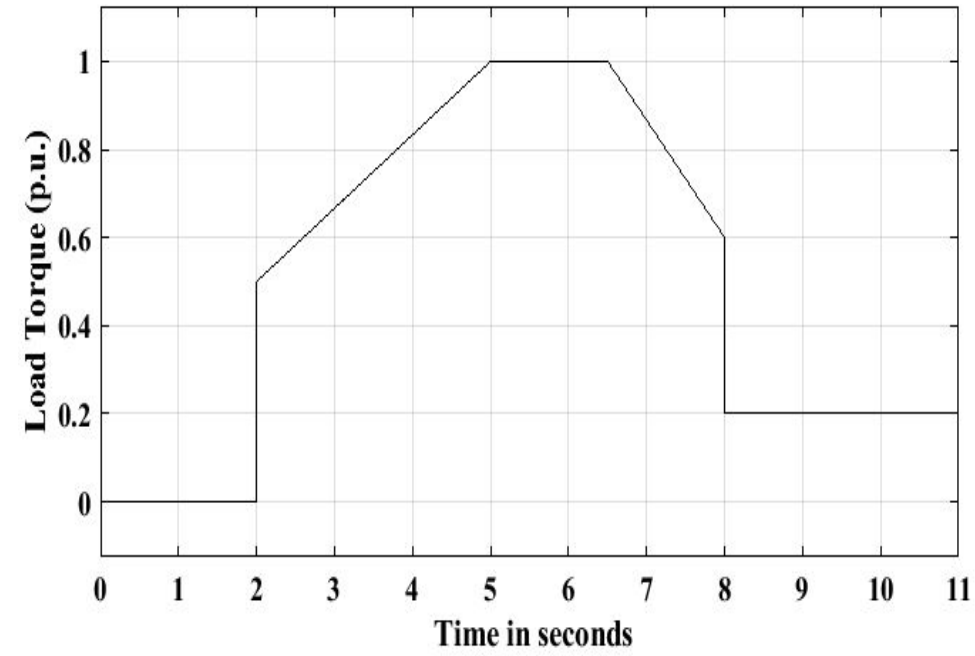

Figure 15 Torque due to undefined type load pattern-1

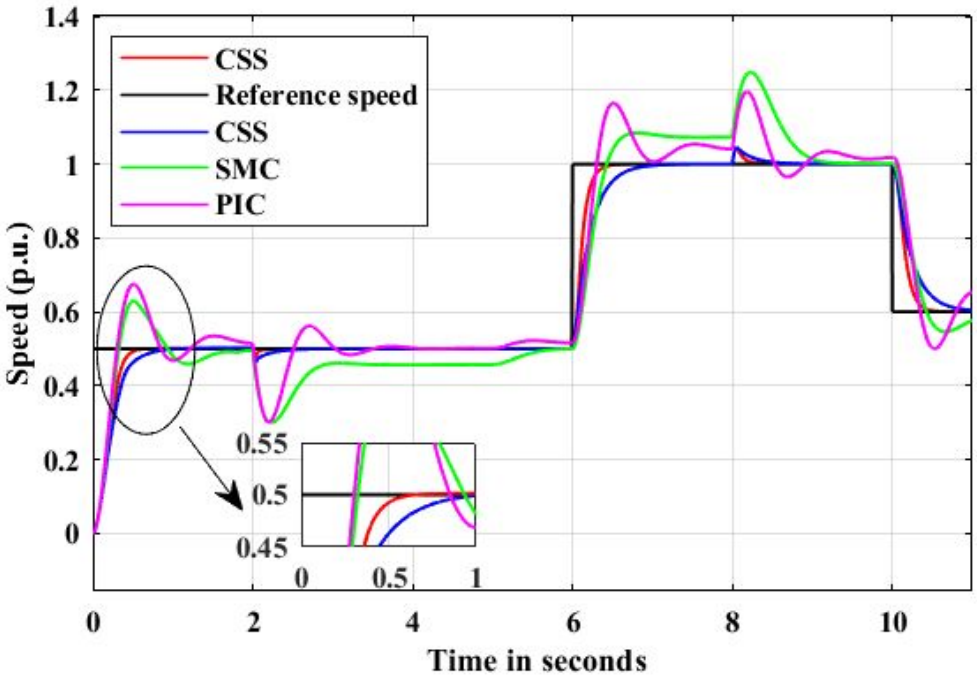

Figure 16 Speed response estimation of PIC, SMC, second order SMC using CSS and PIDSS for the torque due to undefined type load pattern-1

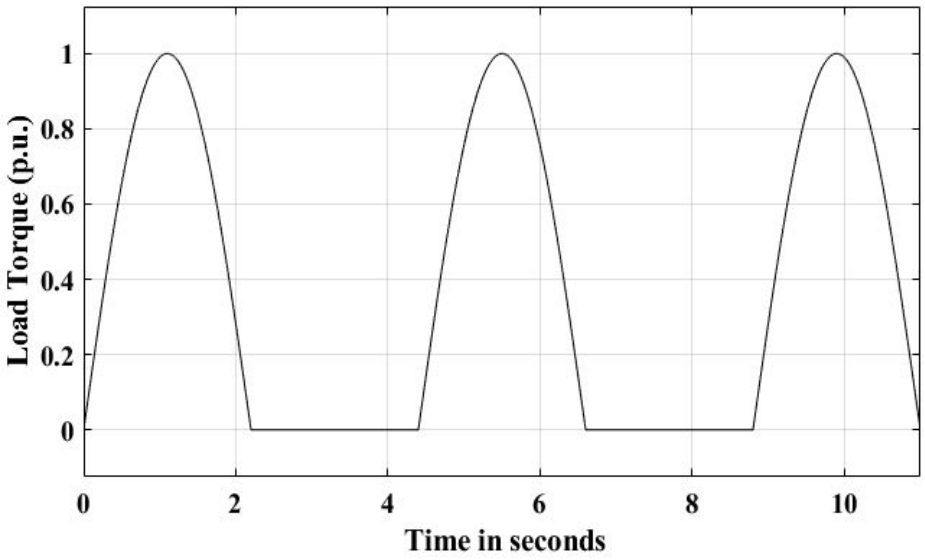

Figure 17 Undefined -load torque-2

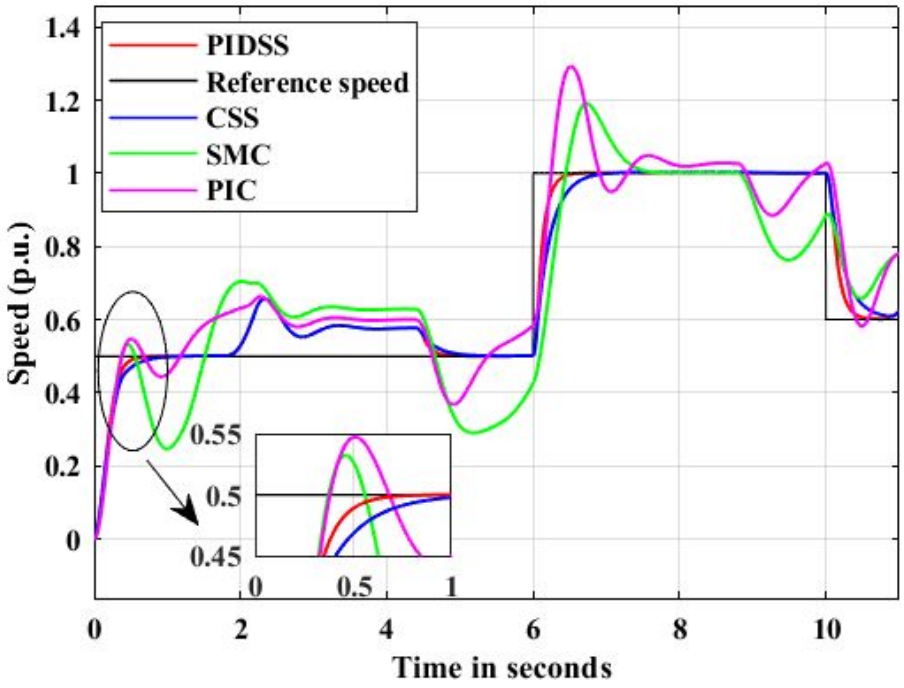

Figure 18 PIC, SMC, second-order SMC using CSS, and PIDSS speed response evaluation for the torque due to undefined type load pattern-2

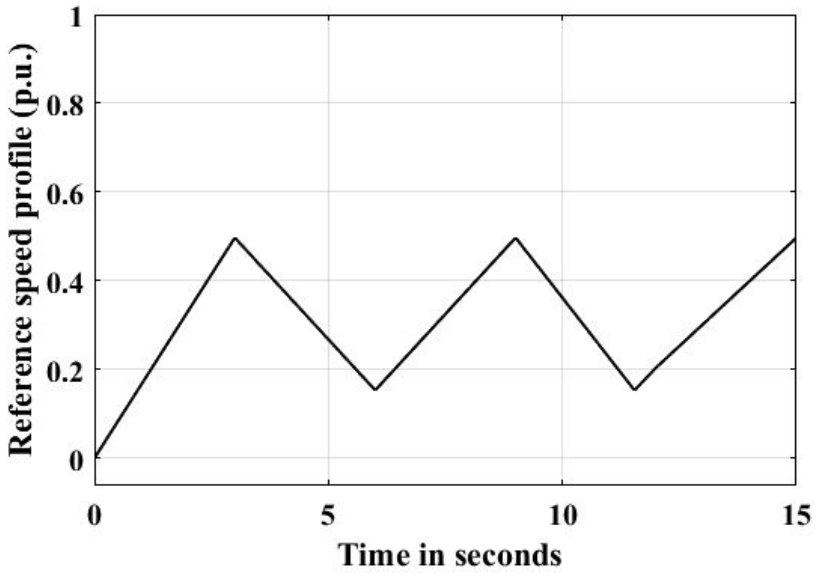

Figure 19 Reference ramp speed pattern

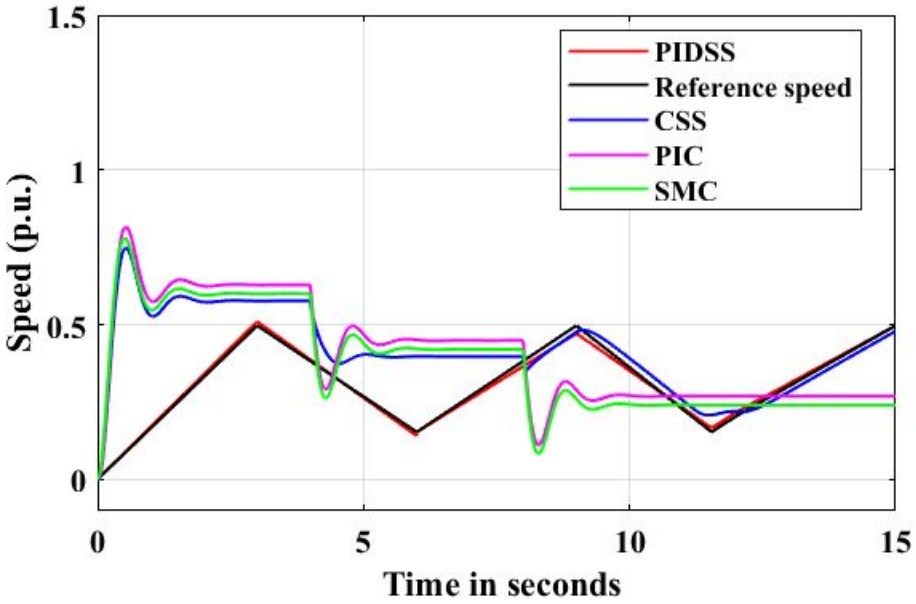

Figure 20 PIC, SMC, second-order SMC using CSS, and PIDSS speed response evaluation for the reference ramp speed pattern

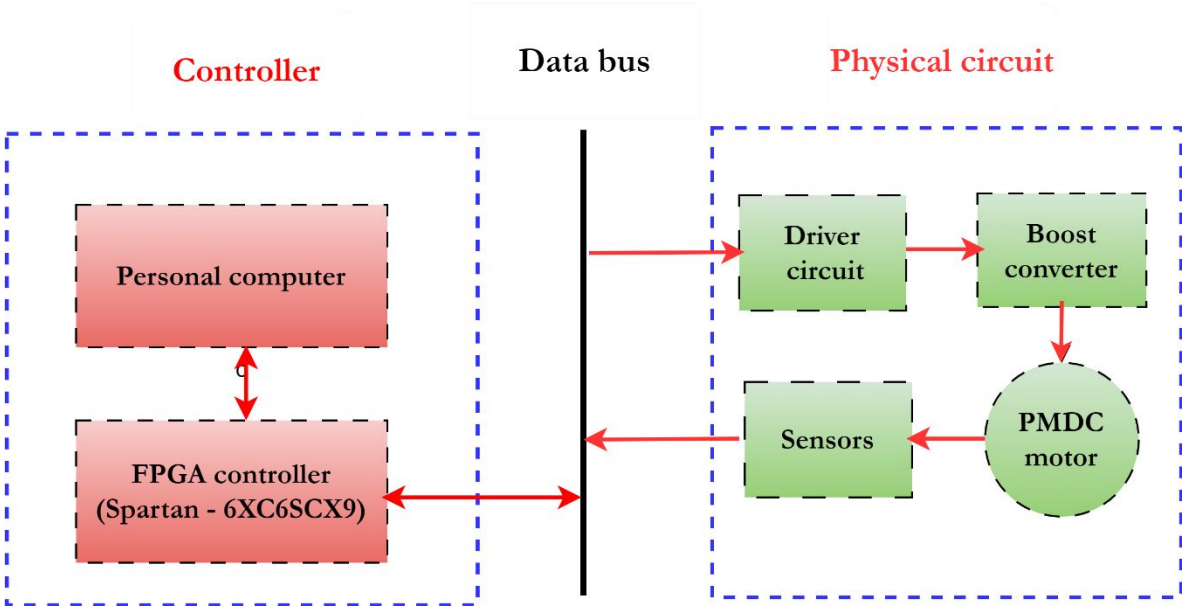

Figure 21 Practical configuration setup

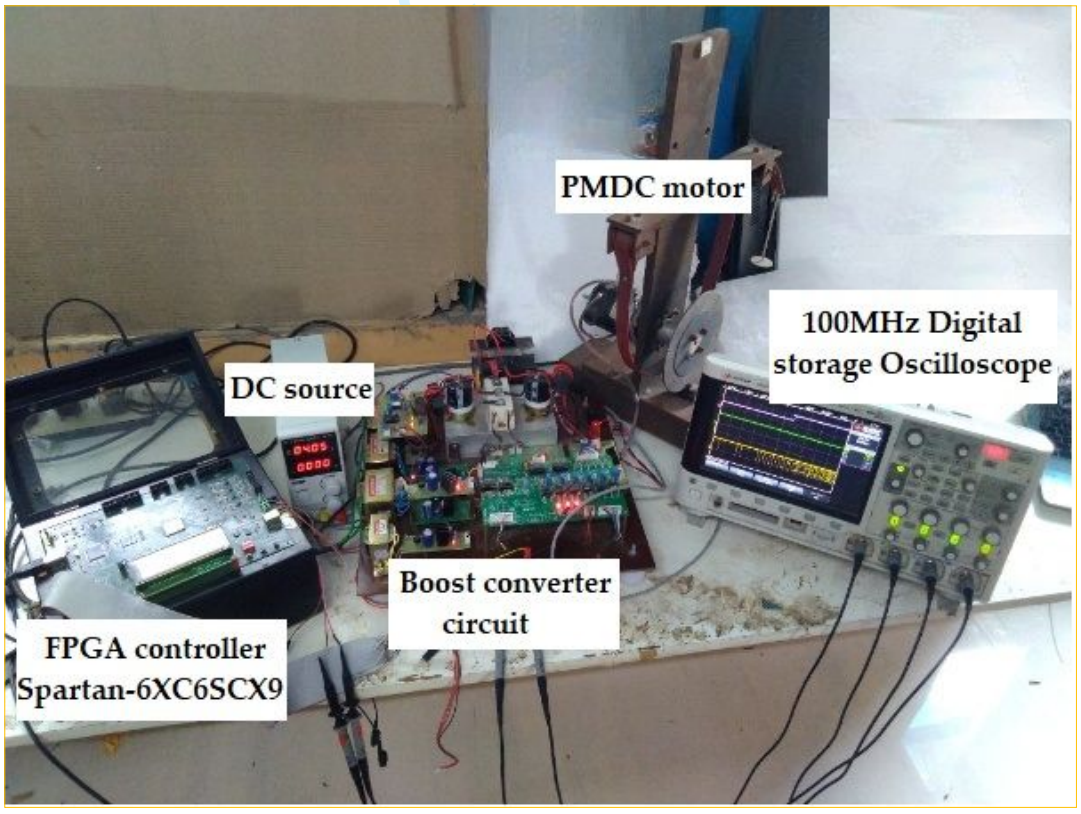

Figure 22 Practical configuration for PMDC motor powered by boost converter

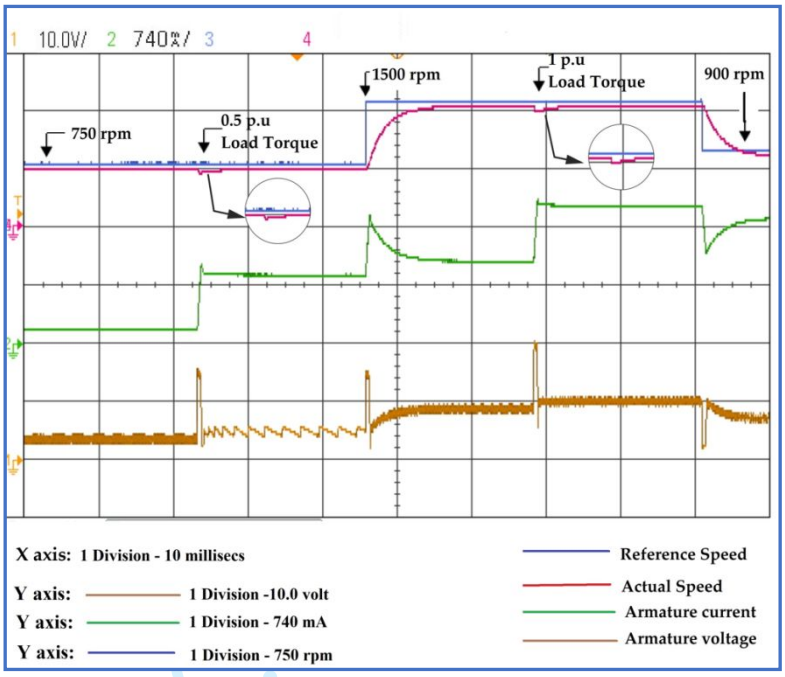

Figure 23 Responses of motor Speed, motor armature current and motor armature voltage changes for second order SMC with CSS

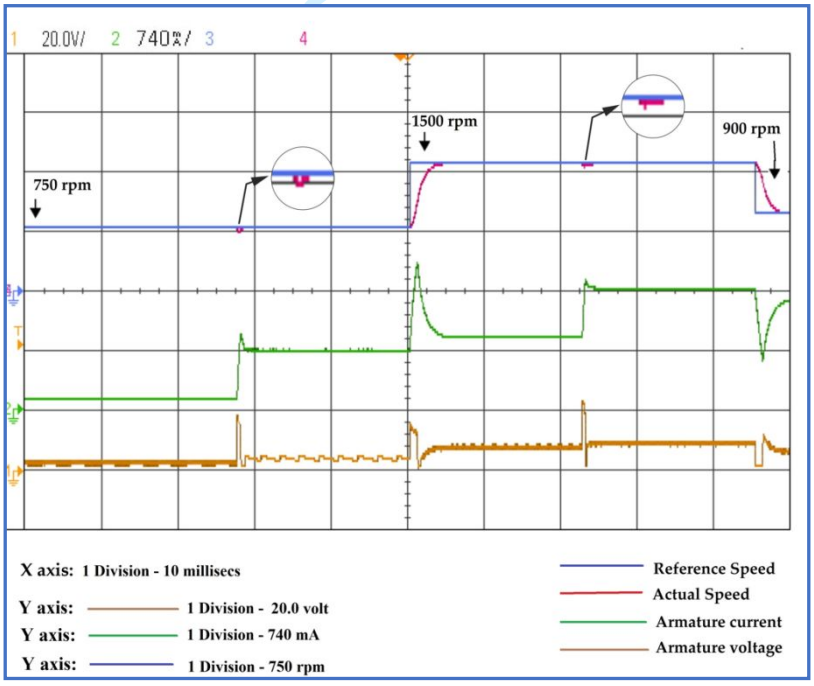

Figure 24 Responses of motor Speed, motor armature current and motor armature voltage changes for second order SMC with PIDSS

Table I. Survey of SMC relating to various applications with challenges addressed

Authors. (Year)	Topology	Type of Sliding mode	Load	Challenges addressed	Disadvantages
Waghmare and Chaturvedi (2023)	Flyback converter	Higher order SMC	Solar PV based applications	Chattering reduction	In comparison to first-order SMC, higher-order SMC may involve a greater control effort (e.g., larger control inputs)
Malge *et al.,* (2023)	Interleaved boost converter	Non-singular fast terminal SMC	Resistive load	Voltage regulation under disturbances	More complex to design and implement in comparison with traditional SMC. It requires a deeper understanding of system dynamics
Rivera *et al.,* (2023)	boost converter	second order SMC	Resistive load	Robust performance under parameter variations	Selection of perfect gains can be difficult and time-consuming
Zambrano-Prada *et al.,* (2023)	boost converter	SMC with polynomial sliding surface	Constant power load	Disturbance rejection, inrush current, stability	Higher computational complexity
Appikonda and Kaliaperumal, (2022)	Dual input boost converter	Double integral SMC	Resistive load	Regulation in voltage under input and load disturbances	Sluggish transient response
Corradini, Ippoliti and Orlando, (2022)	Discontinuous boost converter	Load estimation sliding mode observer	Resistive load	Tested under parameter variations	Low estimation accuracy
Inomoto, Monteiro and Filho, (2022)	boost converter	SMC with integrative sliding surface	Resistive load	Reduces steady state error, peak overshoot	Design complexity
Pandey *et al.,* (2021)	Fuel cell-based boost converter	SMC	PMDC motor	Speed variation	Undesired high frequency oscillations
Wu and Lu, (2019)	boost converter	Adaptive backstepping SMC	Constant power load	Improves the stability of the DC bus voltage	Complex for nonlinear system having coupled dynamics

Chincholkar, Jiang and Chan, (2018)	Cascade boost converter	PWM based SMC	Resistive load	Improves the output voltage response	Selecting an inappropriate frequency may lead to undesirable effects, such as: increased switching losses or harmonic distortion
Aydogmus, Deniz and Kayisli, (2014)	boost converter	SMC	permanent magnet synchronous motor	Power factor correction	Undesired high frequency oscillations
Oucheriah, (2014)	boost converter	Adaptive SMC	Resistive load	Output voltage regulation	Tuning the adaptive laws and control gains
Kumar and Jeevananthan, (2012)	Negative Output elementary boost converter	Hysteresis SMC	Resistive load	Wide variations in line, and load	Introduces nonlinear behavior into the system

Table II. Specifications of boost converter with PMDC motor and the machine behaviour

Parameter	**Symbol**	**Value**
Boost converter input voltage	E	4V
Converter inductance	L	2mH
Converter capacitance	C	1000μF
Converter switching frequency	F	10 kHz
Converter Switch	S	-
Converter Diode	D_D	-
Motor power	P_o	18W
Motor armature voltage	V_a	12V
Motor armature current	I_a	1.5A
Motor torque	T	1 kG.cm
Motor armature resistance	R_a	2.6 Ω
Motor armature inductance	L_a	712.85 mH
Backemf constant	K_e	0.05022 Vs/rad
Moment of Inertia	J	8.86138e-5 kg.m^2
Viscous friction coefficient	B	9.6894e-5 Nm/rad
Torque constant	K_e	0.05022 Nm/A
Speed	ω	157 rad/sec
Machine behaviour		
Time (secs)	**Speed reference pattern (p.u.)**	**Load torque pattern (p.u.)**
0 to 4 seconds	0.5	-
4 to 6 seconds	0.5	0.5
6 to 8 seconds	1	0.5
8 to 10 seconds	1	1
10 to 11 seconds	0.6	1

Table III Comparison of PIC, SMC and second order SMC with CSS algorithm and PIDSS algorithm

Time (secs)	Speed reference (p.u.)	Load torque T_L (p.u.)	Speed - settling duration (secs)				Steady-state error %				Peak overshoot%			
			2nd order				2nd order				2nd order			
			PIDSS	CSS	SMC	PIC	PIDSS	CSS	SMC	PIC	PIDSS	CSS	SMC	PIC
	a) load torque under constant circumstances													
0.0 - 4.0	0.5	0	0.587	0.996	1.563	2.111	-	-	12.5	1.6	-	-	-	17.4
4.0 – 6.0	0.5	0.5	0.091	0.492	1.193	1.901	-	-	-	1.8	-	-	-	8
6.0 -8.0	1	0.5	0.496	1.059	1.532	1.907	-	-	6.7	1.2	-	-	-	16
8.0 -10.0	1	1	0.201	0.555	1.156	1.863	-	-	-	-	-	-	-	7.2
10.0 -11.0	0.6	1	0.476	0.996	Not settled	Not settled	-	-	-	-	-	-	-	-
	b) load torque under frictional type circumstances													
0.0 - 6.0	0.5	0.5	0.699	1.014	1.473	2.377	-	-	-	2.3	-	-	4.5	20.7
6.0- 10.0	1	1	0.501	1.101	1.385	2.250	-	-	-	1.8	-	-	1.3	19.3
10.0- 11.0	0.6	0.6	0.583	1.128	Not settled	Not settled	-	-	-	-	-	-	-	-
	c) load torque under fan type circumstances													
0.0 - 6.0	0.5	0.25	0.516	0.791	1.454	2.155	-	-	-	2	-	-	-	19.4
6.0 - 10.0	1	1	0.571	1.130	1.387	2.254	-	-	-	2.1	-	-	-	21.2
10.0- 11.0	0.6	0.36	0.618	1.209	Not settled	Not settled	-	-	-	-	-	-	-	-
	d) load torque under propeller type circumstances													
0.0 - 6.0	0.5	0.125	0.705	1.122	1.433	2.241	-	-	-	2	-	-	9.8	17.8
6.0 - 10.0	1	1	0.524	1.106	1.337	2.246	-	-	-	1.6	-	-	0.9	21.7
10.0- 11.0	0.6	0.216	0.681	1.154	Not settled	Not settled	-	-	-	-	-	-	-	-

Table IV. Comparative analysis of PIC, SMC and second order SMC using CSS and PIDSS under the torque due to undefined type load pattern-1

Time (secs)	Speed reference changes (p.u.)	Changes in load torque (p.u.) and speed reference (p.u.)	Speed settling time (seconds)			
			2nd order			
			PIDSS	CSS	SMC	PIC
0.0 - 6.0	0.5	i) 0.5 p.u. speed reference at 0 p.u. load torque for 0 to 2 seconds	0.665	0.957	1.671	1.916
		ii) 0.5 p.u. to 1 p.u. of load torque between 2 and 5 seconds of speed reference.	0.098	0.350	1.490	2.168
6.0 - 10.0	1	6 to 10 seconds Load torque varies as 1 p.u. to 0.2 p.u.	0.476	1.004	1.330	1.842
10.0 -11.0	0.6	0.2p.u load torque for the speed reference of 0.6 p.u. from 10 to 11 seconds.	0.547	1.083	Not settled	Not settled

Table V Comparison of PIC, SMC, second order SMC with CSS and PIDSS the torque due to undefined type load pattern-2

Time (secs)	Speed reference (p.u.)	Settling duration of speed (secs)			
		2nd order			
		PIDSS	CSS	SMC	PIC
0.0 - 6.0	0.5	0.382	0.972	-	-
6.0 - 10.0	1	0.327	0.980	-	-
10.0 - 11.0	0.6	0.406	0.846	-	-

Table VI Comparison of second order SMC with CSS and PIDSS in practical configuration for the torque at constant load situation

Variations in Speed reference (rad/sec)	Variations in Speed reference (p.u.)	Load Torque T_L (p.u.)	Settling time of speed (seconds)	
			2nd order	
			PIDSS	CSS
78.5	0.5	0.5 p.u	0.25	0.49
157	1	0.5 p.u	0.35	0.65
157	1	1 p.u	0.3	0.6
94.2	0.6	1 p.u	0.25	0.55